12-19-2022

Establishing Parameters for Selecting Eligible Neutral Current Neutrino-Proton Elastic Scattering Events using MINERνA Detector Samples

Amelia Genus
amg1654@rit.edu

ROCHESTER INSTITUTE OF TECHNOLOGY

Establishing Parameters for Selecting Eligible Neutral Current Neutrino-Proton Elastic Scattering Events using MINERνA Detector Samples

by

Amelia Genus

A thesis submitted in partial fulfillment for the
degree of Master of Science in Physics

in the
School of Physics and Astronomy
Advisor: Dr. Aaron McGowan

Rochester Institute of Technology
Rochester, NY

December 19, 2022

Declaration of Authorship

I, Amelia Genus, declare that this thesis titled, "Establishing Parameters for Selecting Eligible Neutral Current Neutrino-Proton Elastic Scattering Events using MINERνA Detector Samples" and the work presented in it are my own. I confirm that:

- This work was done wholly or mainly while in candidature for a research degree at this University.
- Where any part of this thesis has previously been submitted for a degree or any other qualification at this University or any other institution, this has been clearly stated.
- Where I have consulted the published work of others, this is always clearly attributed.
- Where I have quoted from the work of others, the source is always given. With the exception of such quotations, this thesis is entirely my own work.
- I have acknowledged all main sources of help.
- Where the thesis is based on work done by myself jointly with others, I have made clear exactly what was done by others and what I have contributed myself.

Signed: _____

Date: _____

ROCHESTER INSTITUTE OF TECHNOLOGY

Abstract

Advisor: Dr. Aaron McGowan
School of Physics and Astronomy

Master of Science

by Amelia Genus

The neutrino has been a theorized particle since the early 1900's but its elusive nature has made detecting, understanding, and characterizing it particularly difficult. Experiments to detect neutrinos aim to better discern how this Standard Model particle interacts with matter, its own unique properties, and its ties to the history of our universe. The MINVERνA collaboration studies scattering cross sections by using five different nuclear targets (water, carbon, iron, helium, and lead) to gain a wide array of data involving a range of interaction types. These precision measurements directly reduce the systematic uncertainties for larger neutrino experiments that search for neutrino oscillations (such as NOνA and DUNE). Through this thesis, we aim to study MINERνA data to estimate parameters needed to construct an experimental cross-section for neutral current (NC) elastic neutrino-proton scattering events. We examine events within the 100 MeV to 10 GeV energy range as this contains the highest probability for the desired interaction. We create criteria for differentiating between neutrino-proton versus neutron-proton events to construct a Python script for selecting eligible NC scattering events.

Acknowledgements

First, and foremost, I owe gratitude to Dr. McGowan for guiding me through my research and for aiding my ambitions. Thank you to my family for being a pillar of support through my years of schooling; for constantly being available for advice, wisdom, and as a foundation as I've pursued my academic goals. Thank you to my friends and rowing team that have helped me grow throughout my college experience and for always pushing me to be the best version of myself. Finally, thank you to the physics department for cultivating a positive, challenging learning environment and for making RIT feel like home. No one exists in a vacuum, so it is important for me to recognize the individuals and groups that made my journey towards this accomplishment possible. Thank you.

Contents

List of Figures

List of Tables

Abbreviations

CC	**C**harged **C**urrent
DCS	**D**ifferential **C**ross-**S**ection
FHC	**F**oward **H**orn **C**urrent
GENIE	**G**enerates **E**vents for **N**eutrino **I**nteraction **E**xperiments
GWS Theory	**G**lashow **W**einberg **S**alam Theory
ICS	**I**ntegrated **C**ross-**S**ection
ID	**I**nner **D**etector
HEP	**H**igh **E**nergy **P**article
MC	**M**onte **C**arlo
MINERνA	**M**ain **In**jector **E**xpe**R**iment to study ν-**A** interactions
MINOS	**M**ain **IN**jector **O**scillation **S**earch
NC	**N**eutral **C**urrent
NuMI	**N**eutrino at the **M**ain **I**njector Beamline
OD	**O**uter **D**etector
PMT	**P**hoto- **M**ultiplier **T**ube
RHC	**R**everse **H**orn **C**urrent
RME	**R**est **M**ass **E**nergy
SM	**S**tandard **M**odel
QED	**Q**uantum **E**lectro**D**ynamics
QCD	**Q**uantum **C**hromo**D**yanmics

Physical Constants

Speed of Light	c	=	$2.997\ 924\ 58 \times 10^{8}$ m s^{-2}
Charge of Electron	e	=	$1.60217663 \times 10^{-19}$ C
Fine Structure Constant	α	=	7.299×10^{-3}
Weak Mixing Angle	θ_w	=	0.2229 ± 0.0003
Fermi Coupling Constant	G_F	=	1.1663787×10^{-5} GeV^{-2}
Reduced Planck's Constant	$\hbar$	=	6.5821×10^{-16} eV s
Proton mass	m_p	=	938.272088 MeV/c^2
Z Boson mass	m_Z	=	91.19 GeV/c^2

Symbols

A	atomic number
β	beta particle
e^-	electron
i, f subscripts	initial, final
μ	muon
$\mathcal{M}$	mixing matrix
ν	neutrino
Ω	solid angle
π	pion
$\bar{p}$	3-momentum
p	external momentum
Q	4-momentum
q	internal momentum
R_i	rotation matrix
s	spin
σ	cross section
T	kinetic energy
U_{lm}	MNS matrix
X	nuclei symbol
Z	proton number

To my brother, Avery.

Chapter 1

Introduction

1.1 History of Neutrinos and Weak Interactions

Neutrinos were first theorized by Wolfgang Pauli in 1930 after he noticed inconsistencies with conservation of energy, momentum, and angular momentum in the beta decay process.[4] During radioactive beta-decay, the nucleus is transformed and releases an electron as a result:

$$ {}^{A}_{Z}X \rightarrow {}^{A}_{Z+1}X' + e^{-} \tag{1.1} $$

Based on previously known physics of nuclear decay, the energy of the electron produced in this reaction should have a definite value equal to the difference between the energy of the daughter and parent nuclei; this would correctly account for conservation of energy and momentum. In addition to this, the four-momentum of the observed electrons should have a fixed value, independent of other factors; this is shown in Figure 1.1 by the red line. However, in 1914 James Chadwick used a magnetic spectrometer and an electron counter to show that this was not the case. Instead, a smooth spectrum of electron energies were produced, with a limit up to the expected Q value. Many scientists initially disregarded these results, chalking them up to experimental error,

until similar results were reproduced by Ellis and Wooster in 1927. This brought forth the argument that energy was not, in fact, always conserved.[5]

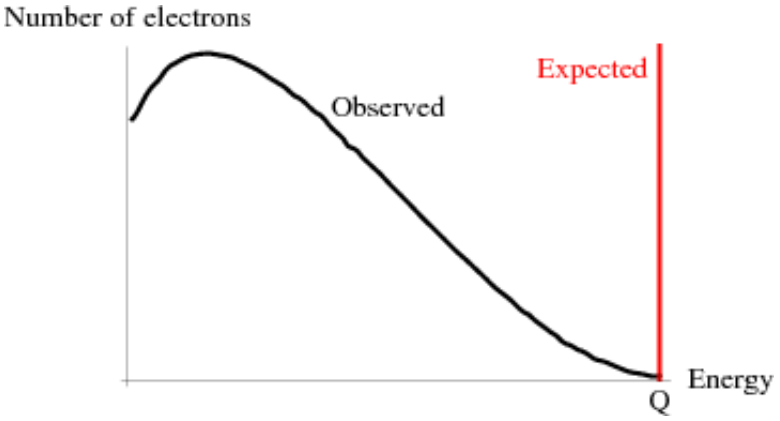

FIGURE 1.1: Beta Decay Energy Spectrum

However, in 1930 Pauli presented a solution to this problem. He proposed that an undetected particle must also be emitted from the nucleus during beta-decay. This new particle must be quite light, similar in mass to the electron, and also be neutral, to agree with charge conservation. Pauli named this proposed particle "neutron" to follow that naming scheme already established. However, after Chadwick's discovery in 1932 of another larger neutral particle, that we now know as the neutron, Enrico Fermi dubbed the smaller of the two "neutrino" meaning "little neutral one."[6] Fermi's work in identifying the process of neutron decay into a proton, electron, and what is now classified as an anti-neutrino worked to combine Pauli's theorized new particle with Dirac's positron and Heisenberg's new model for a nucleus.

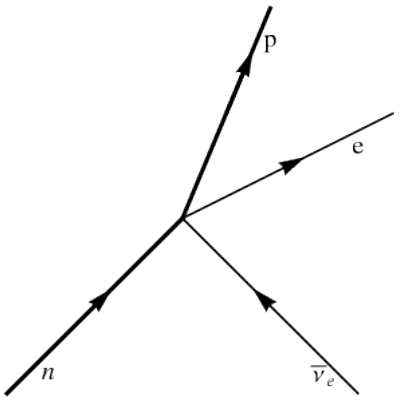

FIGURE 1.2: Beta Decay Feynman Diagram: a neutron and electron anti-neutrino interact producing a proton and electron

When postulating the β-decay process, Fermi based his theory off of the idea that the production of electron-neutrino pairs was analogous to the emission of a photon from an electron. Bethe and Peierls provided the first attempt at calculating an upper bound for the neutrino-nucleus scattering cross-section. However, they found it to be $\sigma < 10^{-44}$ cm^2. From this, they determined there was no feasible way of detecting a neutrino. Despite the overwhelming opinion that neutrinos were an undetectable particle, in 1946 Pontecorvo proposed a radio-chemical method for neutrino detection that later allowed Davis to observe the first ever solar neutrinos: neutrinos born through the process of nuclear fusion within the sun.

The approach to understanding and detecting neutrinos drastically changed in the mid-20th century after the discovery of parity violations in weak interactions. Parity is a way of describing the symmetry of a particle's wave function. For most scenarios the Law of Parity Conservation states that if a group of particles have definite parity, the parity does not change as the group evolves with time. However, it was discovered that in the beta-decay process parity *was not conserved*. This concept of non-conservation of parity in weak interactions was further solidified by what is known as the $\theta - \tau$ puzzle. This puzzle came about as physicists worked to better understand the decay of strange particles. In this puzzle, two seemingly separate particles, θ^+ and τ^+ decay into pions via the following reactions:[7]

$$\theta^+ \rightarrow \pi^+ + \pi^0$$

$$\tau^+ \rightarrow \left\{ \begin{array}{l} \pi^+ + \pi^0 + \pi^0 \\ \pi^+ + \pi^+ + \pi^- \end{array} \right\}$$

The two particles had identical mass, spin, charge, etc, but the only difference in the decays was the parity: +1 for θ^+ and -1 for τ^+. Lee and Yang proposed a solution to this puzzle based on the idea of the non-conservation of parity. They concluded that while parity *was* conserved in electromagnetic and strong interactions, there was not

evidence of it being conserved for weak interactions. So θ and τ were actually the same particle, now called the kaon. This better understanding of the weak force would allow for the progress of theory surrounding neutrino interactions.

The unification of the electromagnetic, strong, and weak interactions gave rise to the structure of the current standard model of particle phyics and laid the groundwork for future neutrino theory. After the second World War, Fred Reines built the first neutrino detector. His detector structure was based on the idea that neutrinos could be found if a large enough test mass was placed near an atomic explosion. The goal was to detect inverse beta decay using liquid crystal scintillators[8]: a process that is still used today in experiments like the Super-Kamiokande neutrino detector. The process of inverse beta decay shows the creation of a neutron and positron from the scattering of an anti-neutrino off a proton: $\overline{\nu_e} + p \rightarrow e^+ + n$. This experiment proved even more insightful than originally anticipated since the signal produced indicated that a neutrino source at such high energy as a nuclear explosion was not actually necessary to produce adequate data, and the high background level detected made it clear that cosmic rays interfered with results. This sparked the initiative to house neutrino experiments underground in the future.

Since this first detection of the electron neutrino, similar processes have been used to detect tau and muon neutrinos. These are the three neutrino "flavors", and they come about from their corresponding charged leptons: the electron, the tau, and the muon. These three types are considered the neutrino *flavor* eigenstates, which differ from the neutrino *mass* eigenstates which are instead labeled 1, 2, and 3. The mixing of these mass eigenstates in creation and annihilation combinations is what form the flavor eigenstates and are what give neutrinos their mass. However, not only do neutrino have the mass oscillations, they also exhibit flavor oscillations. This means that a neutrino may vary its type over a period of time, e.g, an electron neutrino may be produced but it later changes into a tau or muon neutrino. These new flavors of neutrinos can be detected in ways analogous to the beta decay process, e.g., the decay of a pion into a muon and a muon anti-neutrino.

There are two main types of neutrino interactions: charged-current (CC) and neutral-current (NC). CC interactions with matter are facilitated by $W^{\pm}$ bosons whereas in NC interactions a neutral Z^0 boson is exchanged. Within these, the interactions can be classified as either elastic or inelastic, depending on if the state of the original nucleon changes in the final product or not. This thesis will focus specifically on mid-energy NC elastic scattering.

1.2 Neutrinos in the Standard Model

The Standard Model (SM) of particle physics characterizes all the known elementary particles and their interactions with one another through the electromagnetic force and the strong and weak forces. SM theory is based on the local gauge group:

$$SU(3) \times SU(2) \times U(1) \tag{1.2}$$

These represent 3, 2, and 1 dimensional matrices, respectively, that describe the different interactions. SU(3) represents *color* symmetry in strong interactions, and SU(2) $\times$ U(1) is for weak isospin-hypercharge symmetry in weak interactions.

In the SM, each flavor of quark has the ability to come in one of three colors: red, blue, or green. And within the SM, the interaction of charged particles is described using quantum electrodynamics, and quantum chromodynamics describes the interactions of colored particles. For each SU(n) matrix the number of gauge bosons associated with it is $n^2 - 1$ and U(1) has one gauge boson. So for the SM there are 12 gauge bosons: eight gluons, W^+, W^-, Z^0, and the photon.[9] Particles made of matter in the SM are called fermions, which are further split into leptons and quarks.When represented in the SM, neutrinos are a neutral and massless particle, however, due to the discovery of neutrino flavor oscillations they must have mass.The final connecting piece in the SM, is the Higgs Boson. This particle integrates the Higgs mechanism which is responsible for the spontaneous creation of particle mass.

	Particles	Interacting Forces
Quarks	u c t d s b	Strong, EM, Weak
Leptons	e^- μ^- τ^- ν_e ν_μ ν_τ	EM, Weak Weak

TABLE 1.1: Elementary particles and their interacting forces

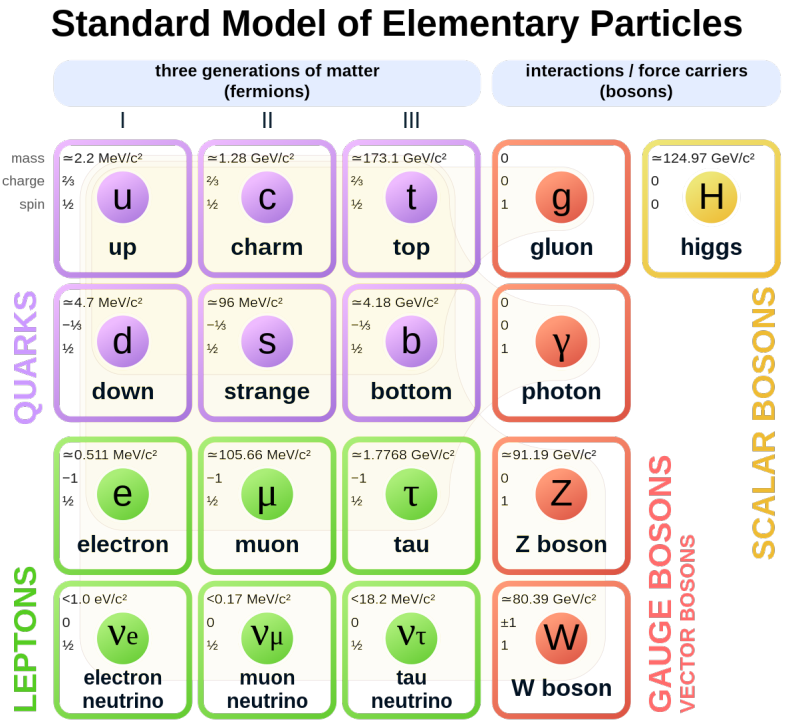

FIGURE 1.3: SM layout showing the grouping of particles [1]

1.3 Neutrino Oscillations and their Mass

As previously mentioned, neutrino oscillations were first theorized by Pontecorvo. The idea was that neutrinos that were created with a specific lepton flavor: electron, muon, or tau, could be measured later to have a different flavor. To understand the origin of neutrino mass from flavor oscillations, first consider that the flavors themselves are manifestations of flavor *eigenstates*, ν_l, where l corresponds to the flavor of the associated charged lepton. Now, assume neutrinos also have *mass* eigenstates, ν_m, different from the *flavor* eigenstates, and that the flavor states are generated through the coherent superposition of the mass states:[10]

$$\nu_l = \sum_{m=1}^{3} U_{lm}\nu_m, \quad l = e, \mu, \tau \tag{1.3}$$

Here U_{lm} is the Maki-Nakagawa-Sakata matrix, which includes mixing angles, charge-parity contributions, and Majorana phases. The complexities of this mixing matrix, while interesting, do not need to be discussed in detail for this thesis.

Chapter 2

Neutrino Scattering Theory

2.1 Background

Despite being proposed over a century ago, neutrino detection proved to be particularly difficult due to their light mass and chargeless nature. In order to fully understand the particle, and the way it interacts with matter, its intrinsic and extrinsic properties must be found and studied. In the future, neutrino experiments such as DUNE (Deep Underground Neutrino Experiment) and Hyper-Kamiokande aim to more precisely measure quantities such as the neutrino mass oscillations. But in order to design effective detector instrumentation and accurately interpret the results, more information needs to be known about neutrino-nucleon interactions. As briefly discussed in the Introduction there are numerous variations of neutrino-nucleus scattering setups. And for many already running experiments, the ultimate goal is to characterize and measure the differential and integrated scattering cross-sections (DCS and ICS) of the different reactions. For example, the COHERENT collaboration aims to detect coherent elastic neutrino-nucleus scattering (CEvNS) which only exists in the low energy part of the spectrum.

Independent of the type of interaction, when neutrinos interact with nuclei they transfer energy and momentum. For CC interactions, a $W^{\pm}$ boson is exchanged while a

charged lepton is produced. However, in NC interaction, when a Z^0 boson is exchanged, the neutrino is present in both the initial and final state. In order to establish a complete understanding of neutrino-nucleus interactions, both NC and CC processes should be studied.

Of the two, NC interactions are particularly difficult to characterize since the predicted cross-section is smaller than that of CC interactions, and the only detectable products of a NC process are either the target recoil energy or the reaction products. Whereas the charged lepton produced in CC interactions is much easier to detect. This paper aims to characterize the background and cross-section for NC neutrino-nucleus interactions at specifically the mid energy part of the spectrum, 100 MeV to 10 GeV. This range was chosen since few analyses have been done focusing specifically on this energy domain. Figure 2.1 shows neutrino cross-section with respect to incident neutrino energy. As shown, MINERνA has collected data in about the 1-50 GeV range which contains mostly resonant and deep-inelastic scattering but at the lower end also contains a small portion of the quasi-elastic interactions.

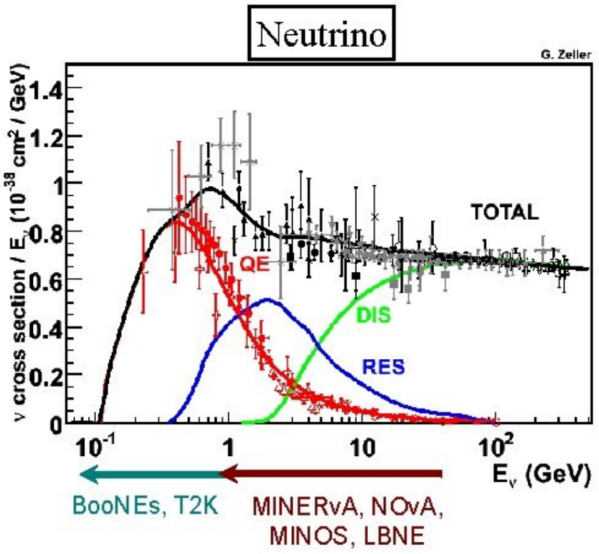

FIGURE 2.1: Scattering Cross-section of Interactions at various energies[2]

2.2 CC and NC Scattering Introduction

When exploring the two types of neutrino interactions, first principles of particle and scattering physics should be defined. While the analysis of this paper focuses solely on characterizing the *NC* elastic scattering of neutrinos, it is still worthwhile to breakdown both processes for a more complete view. In the below figures are the Feynman diagrams that govern inverse muon decay and the β-decay process, both examples of CC interactions.

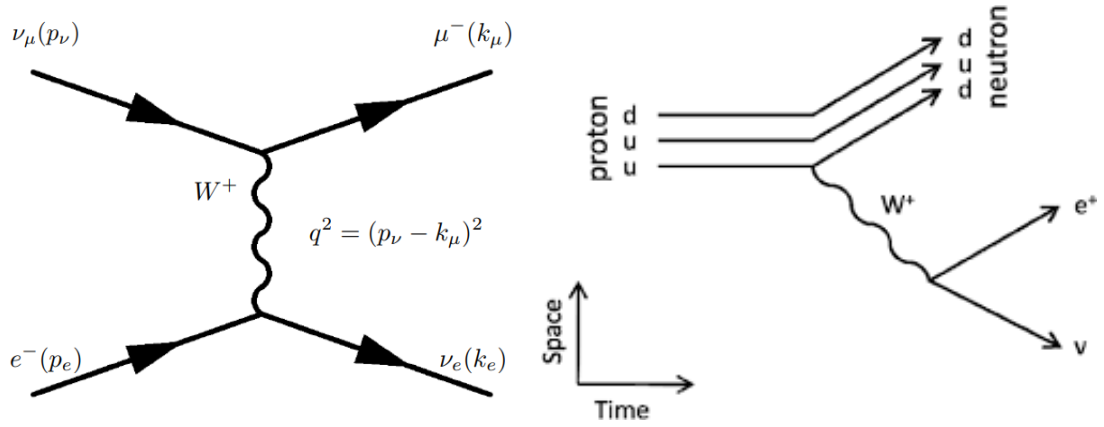

FIGURE 2.2: CC Feynman Diagram for Inverse Muon Decay[2]

The NC scattering processes are another example of how neutrinos interact with matter.

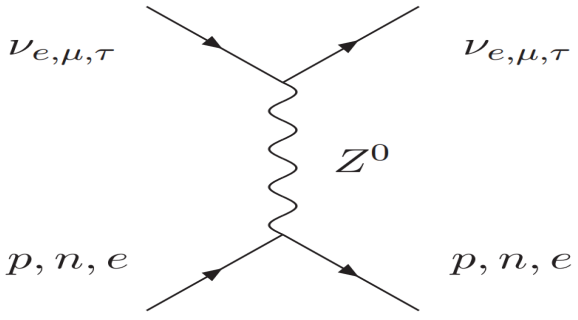

FIGURE 2.3: NC Scattering Feynman diagram

In order to characterize the incident and final state particles, the 4-momentum must be known. 4-Momentum is a matrix that describes the x, y, and z components of a particle's momentum and its relativistic energy. This momentum is the generalization of the classical three-dimensional momentum: $\bar{p} = \begin{bmatrix} p_x, & p_y, & p_z \end{bmatrix}$ into four-dimensional

spacetime. The new momentum vector becomes

$$p = \left[p^0, \quad p^1, \quad p^2, \quad p^3\right] \tag{2.1}$$

where $p^0 \equiv E/C^2$, $p^1 \equiv p_x$, $p^2 \equiv p_y$, and $p^3 \equiv p_z$. So the particles can be defined as:

$$p_\nu = (E_\nu, \bar{p}_\nu)$$

$$k_\mu = (E_\mu, \bar{k}_\mu)$$

$$p_e = (m_e, 0)$$

$$k_e = (E_e, \bar{k}_e)$$

where p represents the momentum of the incoming particles and k is the outgoing momenta.

A full Feynman Dynamics derivation of the process, from the very basics to the full description, can be found in Appendix A: Fundamentals of Feynman Diagram Calculations through Appendix C: Differential cross-section for elastic NC neutrino-proton scattering.

When data is collected in the MINERνA experiment, all 4-momentum vector quantities are established with respect to the detector defined axis but later, axis transformations must be performed to find the vectors with respect to the beam coordinates. As usual, the energy in the vector corresponds to the total particle energy: ${E_i}^2 = {T_i}^2 + m_i c^2$. However, these quantities are Lorenz variant, so when calculated in the cross-section later a Lorenz invariant momentum must be defined: $Q^2 = -q^2 = (p_\nu - k_\mu)^2$, this is the 4-momentum transfer.

In order to obtain elastic scattering, we focus on the mid-energy range (0.1 - 20 GeV). This energy range supports the study of elastic, quasi-elastic, resonance production, and deep inelastic scattering.[11] For NC elastic scattering there are four possible methods in which a neutrino can interact with a nucleon:

$$\begin{array}{c|c} \nu p \to \nu p & \bar{\nu} p \to \bar{\nu} p \\ \nu n \to \nu n & \bar{\nu} n \to \bar{\nu} n \end{array}$$

and to find the differential cross-section, use the below formula:

$$\begin{aligned} \frac{d\sigma}{dQ^2} &= \frac{{G_F}^2 M^2 |V_{ud}|^2}{8\pi {E_\nu}^2}[A + \frac{s-u}{M^2}B + \frac{(s-u)^2}{M^4}C] \\ s - u &= 4ME_\nu - Q^2 - m^2 \end{aligned} \tag{2.2}$$

$$\begin{aligned} A &= \frac{m^2+Q^2}{M^2}[(1+\eta){F_A}^2 - (1-\eta){F_1}^2 + \eta(1-\eta){F_2}^2 + 4\eta F_1 F_2 \\ &\quad - \frac{m^2}{4M^2}((F_1+F_2)^2 + (F_A+2F_P)^2 - \left(\frac{Q^2}{M^2}+4\right)F_P^2)] \\ B &= \frac{Q^2}{M^2}F_A(F_1+F_2) \\ C &= \frac{1}{4}({F_A}^2 + {F_1}^2 + \eta {F_2}^2) \end{aligned}$$

where $\eta = Q^2/4M^2$ and,

$$\begin{aligned} F_1(Q^2) &= \left(\frac{1}{2} - \sin^2\theta_W\right)\left[\frac{\tau_3(1+\eta(1+\mu_p-\mu_n))}{(1+\eta)(1+Q^2/M_V^2)^2}\right] \\ &\quad - \sin^2\theta_W\left[\frac{(1+\eta(1+\mu_p-\mu_n)}{(1+\eta)(1+Q^2/M_V^2)^2}\right] - \frac{F_1^S(Q^2)}{2} \\ F_2(Q^2) &= \left(\frac{1}{2} - \sin^2\theta_W\right)\left[\frac{\tau_3(\mu_p-\mu_n)}{(1+\eta)(1+Q^2/M_V^2)^2}\right] \\ &\quad - \sin^2\theta_W\left[\frac{\mu_p+\mu_n}{(1+\eta)(1+Q^2/M_V^2)^2}\right] - \frac{F_2^S(Q^2)}{2} \\ F_A(Q^2) &= \frac{g_A\tau_3}{2\left(1+Q^2/M_A^2\right)^2} - \frac{F_A^S(Q^2)}{2} \end{aligned}$$

Here τ_3 can take the value of +1 for proton scattering and -1 for neutrons. The strange axial form factor is determined by:

$$F_A^S(Q^2) = \frac{\Delta s}{(1+Q^2/M_A^2)^2}$$

and Δs and M_A (the axial mass) have been found experimentally to be, respectively, -0.15±0.09 and 1.06±0.05 (BNL E734) and 0.08±0.26 and 1.36±0.11 (MiniBoonE).[2]

From Berestetskii et al.[12], a textbook on relativistic quantum theory, the most basic form of the differential cross-section of neutrino-lepton scattering takes the form of:

$$\frac{d\sigma}{dq^2} = \frac{1}{16\pi}\frac{|M|^2}{(s-(M+m_\nu)^2)(s-(M-m_\nu)^2)} \tag{2.3}$$

where $\hbar = c = 1$. And the Jacobian used to transform from energy to angle based cross section is:

$$\frac{dq^2}{dcos\theta_\mu} = 2|p_\nu||k_\mu| \tag{2.4}$$

Within Equation 2.2, the variables s, u, and t are referred to as the Mandelstam Variables. To work through the definitions of these variable, start by simplifying the idea of a scattering interaction. Broken down into the most basic representation, in this case, the interaction of neutrinos with protons is just the elastic collision of two objects with each other. Since this type of interaction is so common in physical phenomena that the Mandelstam variables were developed as a shorthand to express all the necessary kinematics of the collision. Letters s, u, and t are defined as:

$$\begin{aligned} s &= (p_1+p_2)^2c^2 = (p_3+p_4)^2c^2 \\ u &= (p_1-p_4)^2c^2 = (p_3-p_2)^2c^2 \\ t &= (p_1-p_3)^2c^2 = (p_4-p_2)^2c^2 \end{aligned} \tag{2.5}$$

Again, these are the *four-momenta* of each particle in the system. The Feynman Diagrams that will represent this process can then be categorized into s-channel, u-channel, and t-channel interactions. The variables are useful because they are inherently Lorenz invariant, and can easily describe any two-body collision.[7]

Any two-body interaction can be visualized using the primitive schematic below:

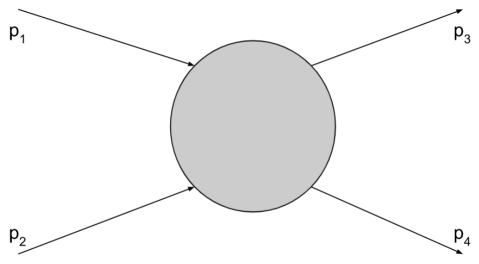

Here, particles 1 and 2 undergo some sort of interaction and out come particles 3 and 4. Further classifying the process types can be done by illustrating the three possible ways that particles 1 and 2 can interact.

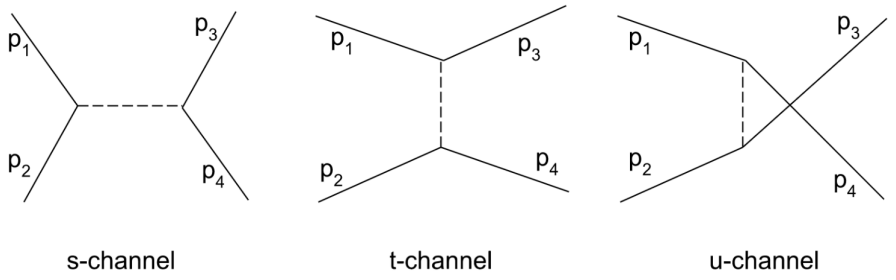

Thus allowing the cross-section expression to be written more succinctly and in a way that is Lorenz invariant. In the case of this thesis, the interaction studied falls into the *t-channel* category.

2.3 Electro-Weak Interactions

The electroweak force is the combination of two of the fundamental forces: electromagnetism and weak interactions. Theory suggests that above a certain energy threshold ($\sim$246 GeV) the two forces act as one. In the 1960s, Glashow, Weinberg, and Salam provided groundbreaking insight to the unification of the two forces and its application to elementary particle interactions. The Glashow-Weinberg-Salam (GWS) theory explains the broken SU(2)$\times$U(1) symmetry that predicts the massive W and Z bosons. Similar to standard weak interactions, in the GWS model there are both charged and neutral electro-weak interactions.

In this thesis, the scattering of neutrinos on protons is investigated. However, in order to characterize the formula for the scattering cross-section, differential or otherwise, the interaction must be broken down further. This process is simply the scattering of a lepton (the neutrino) off of a collection of quarks (the proton).

The formalism of both weak and electro-weak interactions rest upon the idea of symmetry. Similarly to the strong force, the weak force is short-range acting with the

range being around 10^{-15} cm. But differing from the strong force, weak interactions are caused by symmetry spontaneous breaking, which gives rise to the massive W and Z bosons.

To understand how this symmetry can be broken, it is necessary to understand the difference between *global* symmetry versus *local* gauge symmetry. Gauge symmetry, or gauge invariance, refers to when the measurable or observable quantities of a field remain constant under a configuration change. Local symmetry A global symmetry is simply a local symmetry that is fixed at all points of spacetime

is what allows photons and gluons to be massless, so the only explanation for the massive mediator particles is *local* gauge symmetry being spontaneously broken. The Goldstone theorem states that a Goldstone boson, with no mass and zero spin, is assigned to every broken global symmetry group. For the global U(1) group, the ground state is not invariant under an infinitesimal transformation so there is broken symmetry. Again in the U(1) case, if switched from global to local symmetry the assigned Goldstone boson gains mass through its interaction with the gauge field.[13]

In the GWS theory, the weak interaction is mediated by the $W^{\pm}$ gauge bosons that are massless. Similarly, the lagranian contains elements for massless electrons, muons, and neutrinos. These particles are invariant in the local symmetry group and obey gauge symmetry. Next, the Higgs field (a scalar field) is introduced which results in spontaneous symmetry breaking. This allows electrons, muons, taus, and gauge bosons to have mass, however not photons or neutrinos. Within this process, the Z boson and the photon are generated by different combinations of the same two gauge fields: one results in the massless photon, the other combination allows the Z boson to have mass.

The masses of the W and Z bosons can be determined using experimentally well-known values: the Fermi coupling constant (G_F), the weak mixing angle (θ_w), and the fine structure constant (α):

$$m_W = (\frac{\alpha\pi}{G_F\sqrt{2}})^{1/2}\frac{1}{sin(\theta_w)} \qquad m_Z = (\frac{\alpha\pi}{G_F\sqrt{2}})^{1/2}\frac{2}{sin(2\theta_w)} \tag{2.6}$$

where $G_F = 1.66 \times 10^{-5}$ GeV^{-2} , $\sin^2\theta_w = 0.235 \pm 0.005$, and $\alpha = 1/137.04$.

This explanation of how the weak force intermediary particles gain their mass is necessary for constructing the final expression for the scattering cross-section.

Chapter 3

MINERvA Detector and Experiment

The Main Injector Experiment to study ν-A interactions (MINERνA) is housed at Fermi National Accelerator Laboratory (Fermi Lab) and is the first high-intensity beam to study neutrino interactions with five different materials: water, helium, carbon, iron, and lead. MINERνA's location and unique detector design makes it significantly different than other neutrino beam experiments, and its main goal is to study neutrino *flavor* oscillations. The goal of understanding how neutrinos morph over time helps to give insight into the conditions of the early universe. In addition, furthering our understanding of neutrinos could prove helpful in studying dark matter and energy, and the questions surrounding why there is more anti-matter than matter in the universe.[14]

3.1 Experimental Design

The high-intensity neutrino beam is generated at the main injector beamline (NuMI). The neutrinos are created by bombarding a carbon target with protons; the target is located in a focusing horn that directs the shattered carbon particles into a magnetic field. As the charged particles, mostly made up of pions, travel along the decay pipe they

decay into muons and muon-neutrinos, if positively charged, and anti-muons and muon-antineutrinos, if negatively charged. There is then over 200 meters of rock and particle absorbers that block anything from passing through except for neutrinos. Finally the neutrinos enter a space called the "detector hall"; this contains the experiments MINOS (Main Injector Oscillation Search), NOνA, and MINERνA.

Since neutrinos are neutral particles, their interactions with matter cannot be seen directly in the same way that charged particle interactions can. However, the charged particles emitted from these scattering events are able to be "seen" by common detector instrumentation. Below shows a detail schematic of the MINERνA detector breakdown:

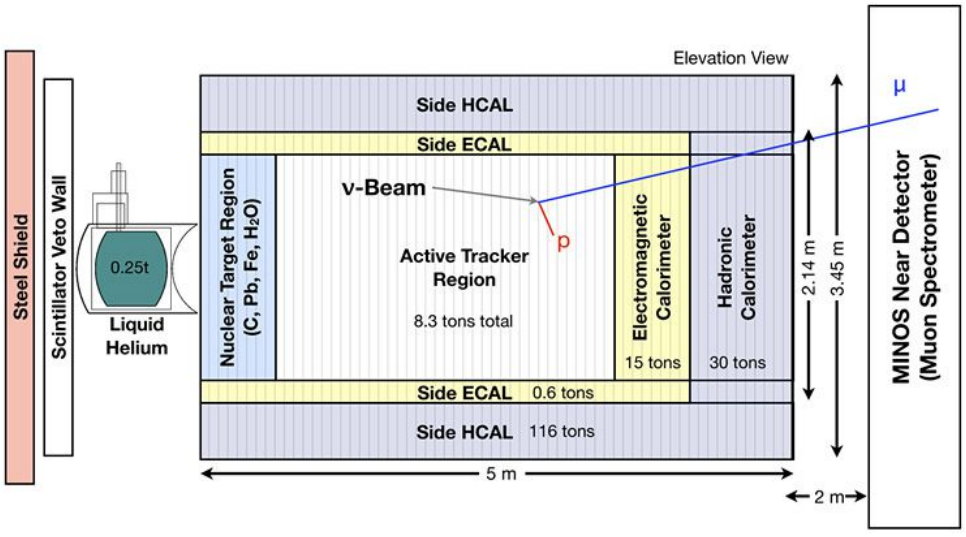

FIGURE 3.1: MINERνA Detector Setup[3]

From left to right: a steel shield; a scintillator veto wall which is used to capture any large hadrons created by a neutrino interaction with the preceding rock and not making it to the main detector region, and also tags any muons coming through as "rock muons;" a cryostat of liquid helium as one of the nuclear target materials; then comes the main body of the detector, which will be explained in more detail in a later section; and continuing down the beamline is the MINOS near detector.[15]

3.2 NuMI Beamline

This beamline produces muon neutrinos and antineutrinos from a 120 GeV proton source bombarding a graphene target to produce pions. These particles enter the target hall where focusing horns are used to funnel them into a beam. The focusing horn can be in one of two orientations: the forward horn current (FHC) or the reverse horn current (RHC). Depending on the type of current in the horn, the beam will consist of mainly neutrinos if in FHC and antineutrinos if in RHC.[16] These pions are allowed to decay into neutrinos within the decay pipe, thus forming a beam of purely neutrinos.[?]

3.3 Main Detector Body

As previously mentioned, the first nuclear target encountered is a cryostat of liquid helium. This is followed by a region of water and then thin sheets of carbon, lead, and iron. The detector is segmented along the main axis into hexagonal sheets. Each sheet contains an inner detector (ID) with the active tracker region made of scintillators, a side electromagnetic and hadronic calorimeter, and an outer detector (OD) made up of scintillators embedded in steel; see Figure 3.2. These sheets are sandwiched together to form the full detector.

The active tracker region performs the pivotal job of measuring energy loss per unit length and the reconstruction of the neutrino interaction vertex. The layers of hadronic and electromagnetic calorimeters serve to contain any hadrons produced in the active tracking region.

From Figure 3.3, the positive y axis is defined straight upward and the positive x-axis is to the left. The z-axis runs along the main detector axis with z=1200m defined to be the front of the MINOS near detector, and the x-y plane origin is at the center of the inner detector. The incoming neutrino beam angle makes a 3.34° angle with the y-z plane which will be important in the later data analysis. Figure 3.2 also shows a side view of the detector, clearly showing the full assembly of all the sheets.

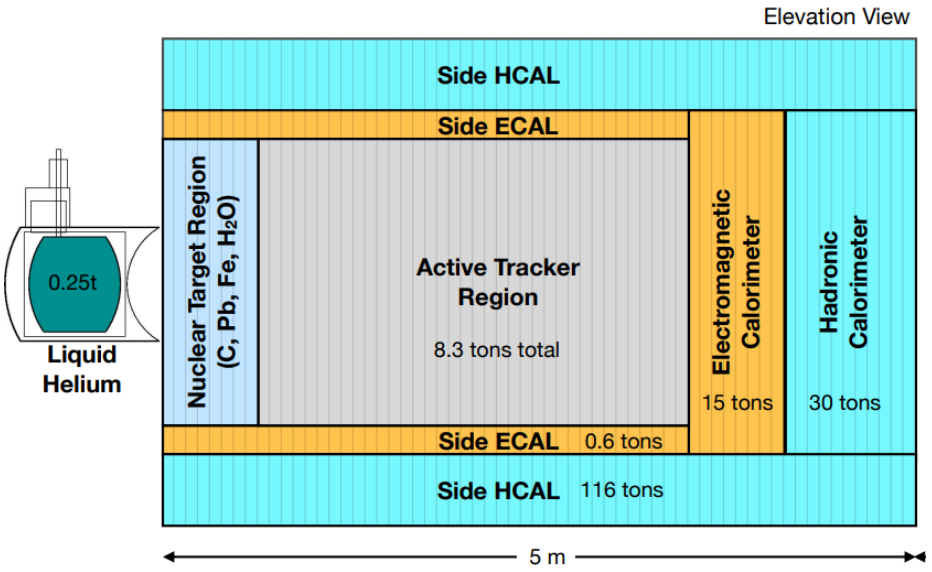

FIGURE 3.2: Main Body

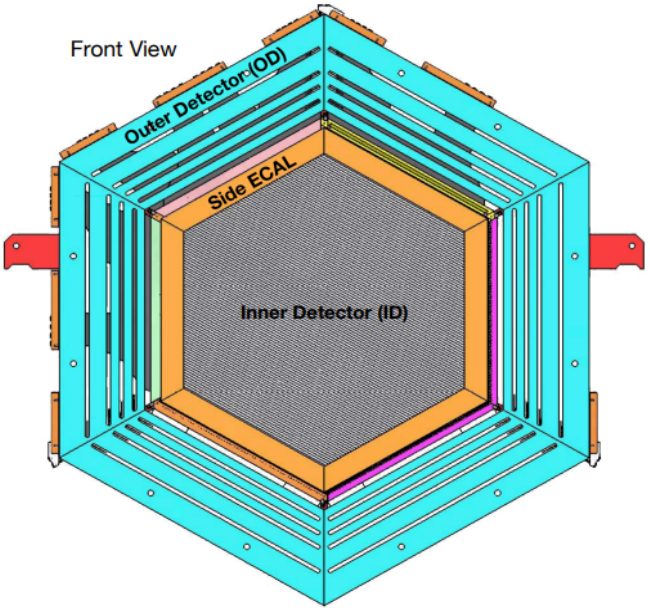

FIGURE 3.3: Detector Cross Section

3.4 Data Collection and Simulation

Over the course of its lifetime, the MINERνA experiment collected 4 x 10^{20} protons on target in the low energy range and 12 x 10^{20} in the mid energy range. The active

tracking region is used to reconstruct neutrino interaction tracks through the detection of the large *charged* hadrons: since neutrinos themselves are neutral and cannot be seen by the detector. The experiment uses a code algorithm called GENIE to model the neutrino interactions and final-state particle interactions are modeled by a GEANT4 simulation. GENIE is a motion control device "designed to capture time-lapse photography and real-time video." Whereas GEANT4 "simulate[s] the passage of particles through matter." In this experiment GEANT4 is specifically used to model the electronics, scintillators, and absorbers of the detector. A much more detailed explanation of the optical setup and data collection and calibration can be found in L. Aliaga, et al.[14]

Later in this thesis, reconstructed muons are used heavily in the analysis, so it is important to review the muon reconstruction algorithms used. The muons used, appear first within MINERνA and continue to travel downstream to be collected in the MINOS near detector. MINOS uses magnetics to determine the charge and energy of the incoming muons.

In order to create reconstructed *events*, numerous parameters must be combined to satisfy specific criteria. Any reconstructed muon track must have a matching one in the MINOS detector: this is so its momentum and energy can be determined, and the vertex needs to be in the active tracker region in the scintillator part of the ID.

3.5 GENIE

GENIE is one of the intermediary steps taken during the data collection process that specifically focuses on the Monte Carlo generated events that are then utilized in the Arachne simulation. The main goal of creating the software package GENIE was so it would become a widely used neutrino event generator that could support interactions with any nuclear target type and any neutrino flavor. It also has the capability to span a wide energy spectrum to better encompass any future neutrino detection experiments; the eventual goal is to be able to support an energy scope of $\sim$1MeV to $\sim$1PeV, but as of right now GENIE only has the capacity to model interactions in the range of $\sim$100MeV

to a few hundred GeV. Previous MC simulations tended to be created by and for each individual neutrino experiment, GENIE was created to be a "canonical" MC neutrino event simulator that could be customized to any experiment's needs and would be able to evolve with any new findings in neutrino physics.[14]

For NC elastic scattering, GENIE uses the model from Ahrens, et al. [9] where the axial form factor is:

$$G_A(Q^2) = \frac{1}{2}\frac{G_A(0)}{(1+Q^2/M_A^2)^2}(1+\eta) \tag{3.1}$$

from this model the default value for η is 0.12.

GENIE is a ROOT-based object orientated software structure, therefore, all information and data is stored in the ROOT tree framework: generated events are stored in GHEP event trees which hold all the information about the generated particles, i.e., 4-momentum transfer, charge, mass, name, position in the detector coordinate system, etc. And these particles can be in the initial, intermediate, or final state. The event record contains *all* the information about a given generated event which is then summarized in the interaction summary. GENIE also has access to ROOT databases to query information about different particles classes like MC PDG codes, names, decay channels, etc.

GENIE modeled interactions create objects that combine initial and final state objects with event kinematics, process type, and any other information associated with such. This interaction object is used to generate the interaction summary object which are then tagged together. After the full process of event generation, GENIE has the capability to be access applications that act as wrappers for the detailed process. There are many different applications that the user can interact with to be able to simulate events. [17]

3.6 GEANT4

Similarly to GENIE, GEANT4 is a C++ script based software system. However, unlike GENIE it was not specially designed for neutrino physics work and has applications in other sectors of HEP, nuclear, space, medical, and accelerator physics.[18] GEANT4 is designed to be both a stand alone event simulator and a software that can be integrated into other frameworks to accomplish simulation desires. This toolkit is comprised of an event generator that houses all necessary kinematics, detector simulation, reconstruction, and analysis. It also has the capabilities to support add-ons to the software to expand its applications. Its main goals are to completely model the particle interactions with nuclear targets and simulate the working detector; to do this it records the detector geometry and materials; it simulates particle interactions with matter and implements pathway tracking; and, it also contains a visualization framework that is built into the easily navigable user interface.

Each of the categories shown in the diagram in Figure 3.4, work together to form the complete GEANT system. Global contains the system of units, physical constants, and the numerics; intercoms is the method that allows the visual user interface to connect with the actual GEANT4 software; the other modules *Material, Particle, and Geometry* contain the geometry of the particle interactions and a detailed description of the detector. These are all built into the module *Track* which is used in conjunction with *Processes* and *Digits+Hits* to form the whole Tracking category. All of the tracked hits are digitized and grouped into Events, these events are grouped together into different runs based on beam and detector implementation.

All of the processes needed to create tracks of interactions rely on the information stored in the *Particles* and *Materials* modules. Particles uses the class G4ParticleDefinition to contain information about particle charge, mass, spin, parity, etc. Within this class there are subsections that classify the particles into leptons, mesons, bosons, baryons, etc. This allows for the implementation of the particle classes within GEANT4. Materials is used to describe the physical properties of compounds, isotopes, single elements,

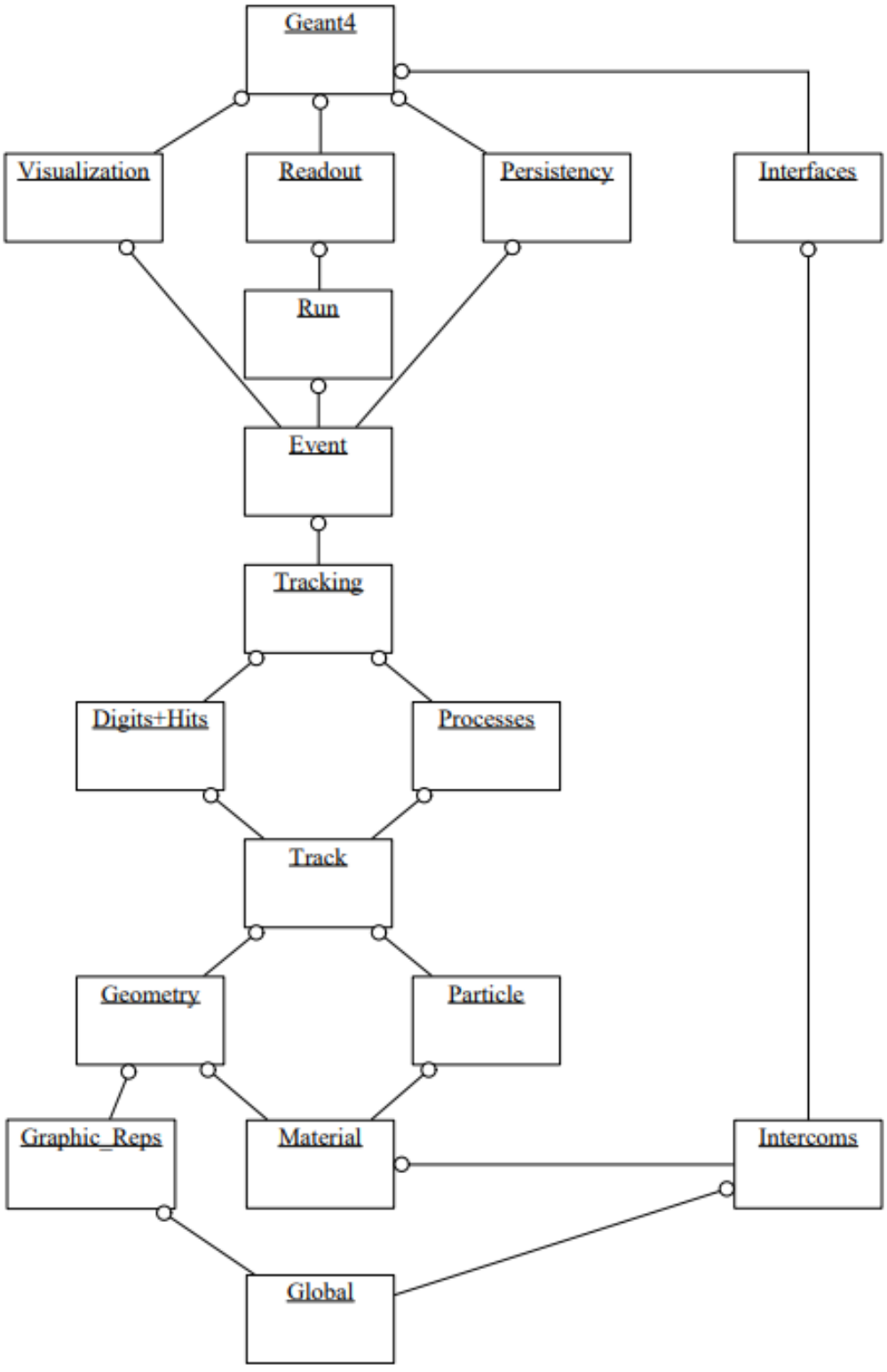

FIGURE 3.4: GEANT4 top-down set up

and contains their radiation, energy loss, interaction length, etc. Materials also can describe surface properties of different components.

The main tracking process is done using a method called *Smart Voxels*. The space is divided into smaller cubic voxels, but unlike the traditional grid structure of ray-tracing voxel methods, the smart voxels used in GEANT4 are divided based on an optimized axis and the subdivided volumes with similar sizes are grouped together to improve memory and performance. These volume boundaries are used in conjunction with calculated trajectories to determine particle propagation. The propagation is done in time-steps using a fourth order Runge-Kutta method, however, this order RK integration works best with fields that are uniform or vary smoothly.

3.7 GAUDI

Just like in any other high energy particle experiment, MINERνA produces millions of raw data points that need to be processed, reconstructed, and analyzed. GAUDI was originally developed for the LHCb experiment to be used as the architecture connecting the event simulation software, high level triggers, and the event visualization software. The goal of GAUDI was to provide an object-oriented framework for subsequent software releases that would be adaptable to new requirements and uses. The adaptability aspect was most important so that it could be expanded to fit needs as they arose, without creating completely new software frameworks for each task, which could lead to duplication and fragmentation of computational effort.[19]

An important aspect of GAUDI is the distinction between *data* objects and *algorithm* objects. GAUDI also chooses to separate *persistent* and *transient* data.

To form the detector description in the framework, GAUDI accesses the detector description from the GEANT4 simulation toolkit. The detector data is stored in the Transient Detector store, which is accessed by the *Algorithms* object. The transient store also contains the logical detector structure, its geometrical elements, and the materials that make up the detector. However, if needed, other aspects can be added. The unique quality of the GAUDI *Algorithms* framework is that the connections between objects in the different categories are only created if and when they are directly being used:

otherwise they do not exist in the memory. This helps with speed of data access and data storage management.[20]

3.8 Arachne

For the visualization of particle tracks and events, the MINERνA collaboration created a web-based tool named Arachne. After the raw data is collected by the detector and put through the GAUDI reconstruction framework, the information is stored in ROOT files in the form of NTuples. When a user wants to view an event, the request accesses the Arachne server and returns the relevant data to the JavaScript user interface for the hit to be displayed. The display features a two-dimensional schematic of the scintillator strips that connect to the PMT's; this shows the individual hits, and some reconstructed tracks from the desired event. There is also the option to display histograms of specified variables, alongside the visual representation of the event. There is also an option for a three-dimensional view of the event, that is implemented using a custom JavaScript library.[21] This visualization software is explained further in the next chapter.

Chapter 4

Arachne Event Display

4.1 Setup

As previously mentioned, Arachne is the primary user interface utilized by MINERνA to view the collected data hits. Each event is stored in the MINERνA database which is used as the input for the display. The graphic includes various modules containing an array of information associated with each event, as well as its Monte Carlo simulated version. Each event is divided into cuts, entries, and slices which can be scrolled through to view each data point. The modules include a time histogram showing the frequency of hits as they enter the detector, PH histogram for displaying the energy spectrum, and the slice info module with a numerical description of each slice.[22]

The most useful part of the visualization is done in the hit maps, big hit map, and 3D display modules. In these, the user is able to see all of the PMT hits within the detector as a function of 2D and 3D space. They also are segmented into the major sections of the detector, so it is easy to understand where the interaction initially takes place, and the effected components. The Monte Carlo module contains the information for the simulation of the event, which can be toggled on and off in the hit maps, to see how closely the actual data matches the simulation.

4.2 Event Characterization

Take for example a DST file from the first subrun; in this case looking at the first entry of the first cut:

FIGURE 4.1: Any stored DST file can be viewed by inputting its path into the Filename search bar

This arachne provides complete slice information breakdown and an energy histogram:

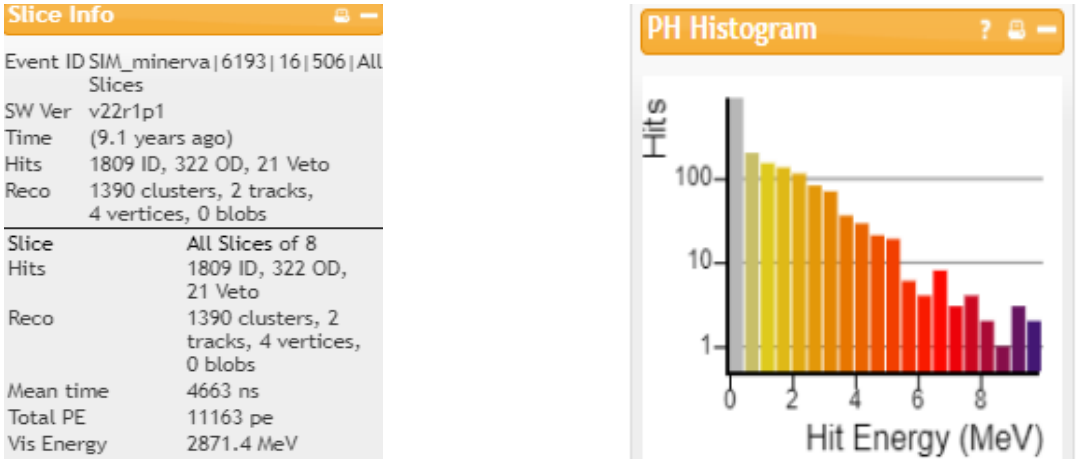

FIGURE 4.2: The slice info module contains information about the chosen DST file, i.e, total slices, length of time, total photo-electrons detected, and all visible energy. The hit energy histogram provides a visual of the number of hits associated with different energy deposits.

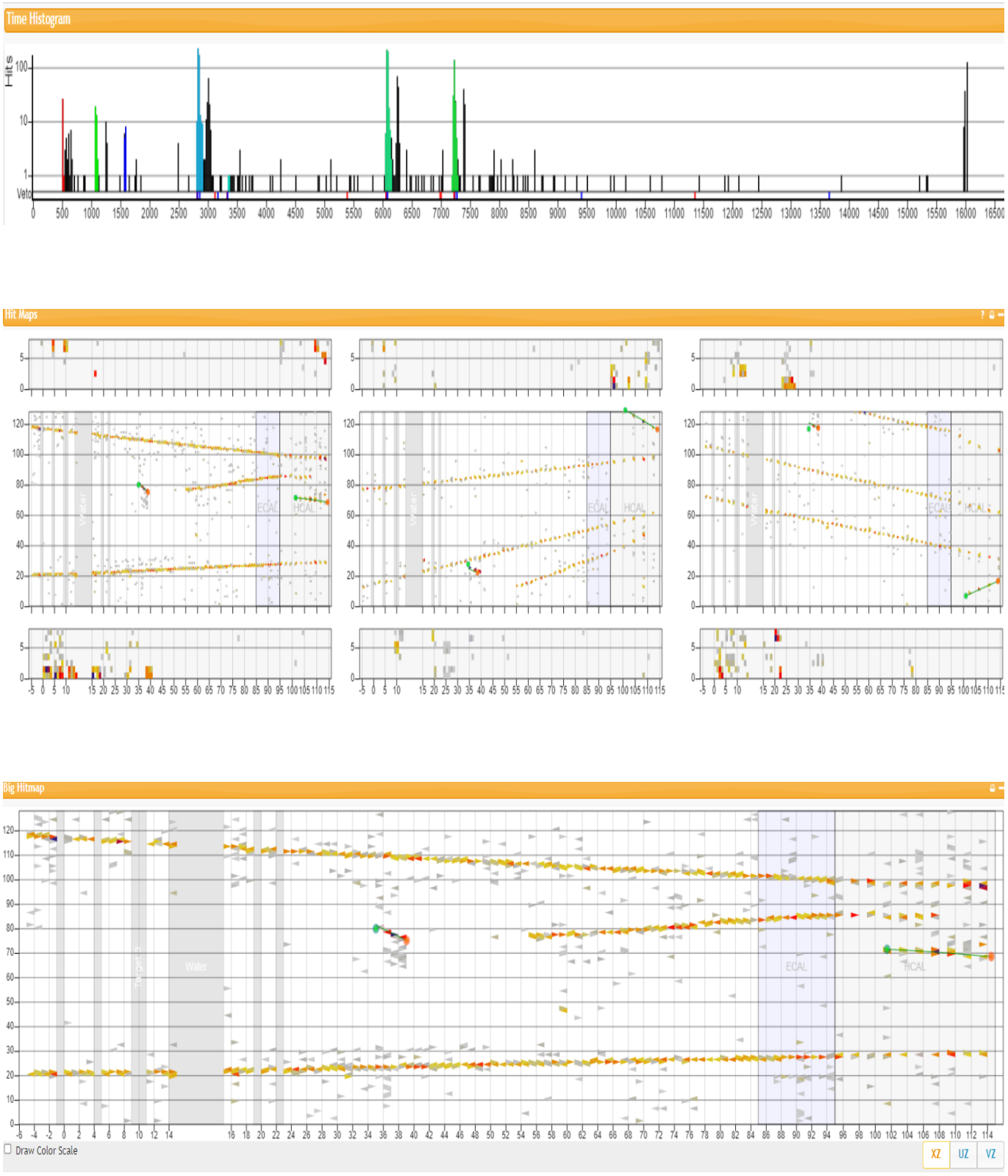

FIGURE 4.3: This entry of the DST files contains four tracked particles that are potentially protons

The Monte Carlo truth information can be viewed in the MC module or the MC Digraph:

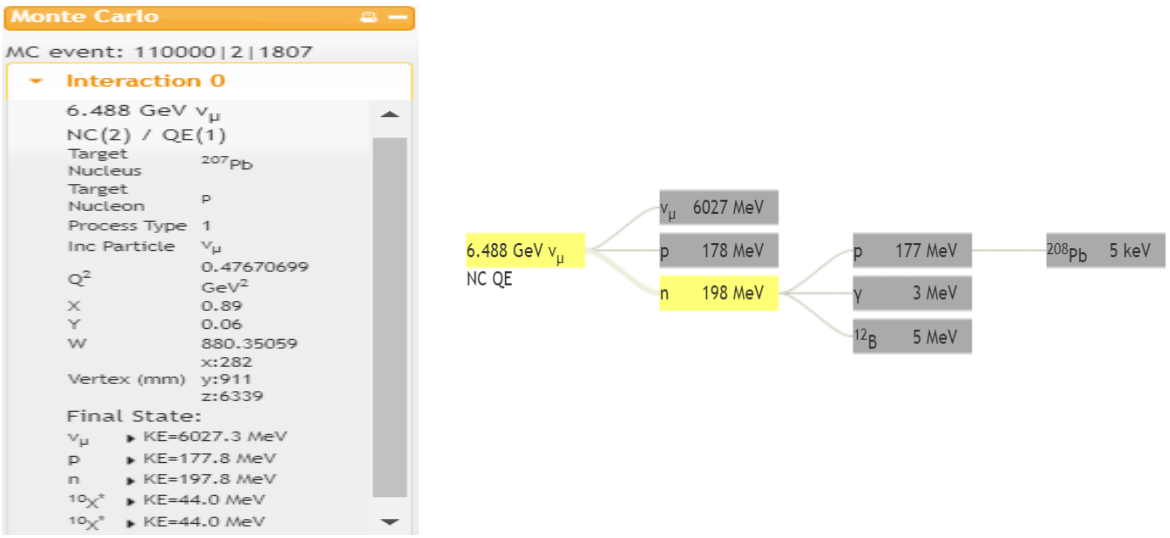

FIGURE 4.4: The MC module provides information about the truth variables of the simulation. This includes incident neutrino energy, final state energies, vertex location, etc. The diagraph shows the scattering progression of the simulated particles

This specific file contains one tracked proton in Slice 1. To investigate this further, Arachne allows the user to scroll through the time slices as well as toggling on and off the MC truths.

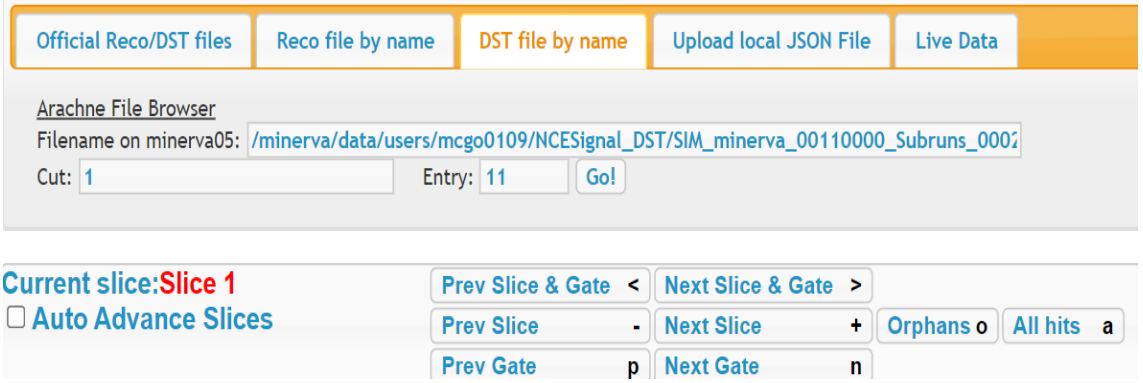

Having the MC truth toggled on, it is easier to get a clearer understanding of what the scintillator hits mean, and where "invisible" particles are going.

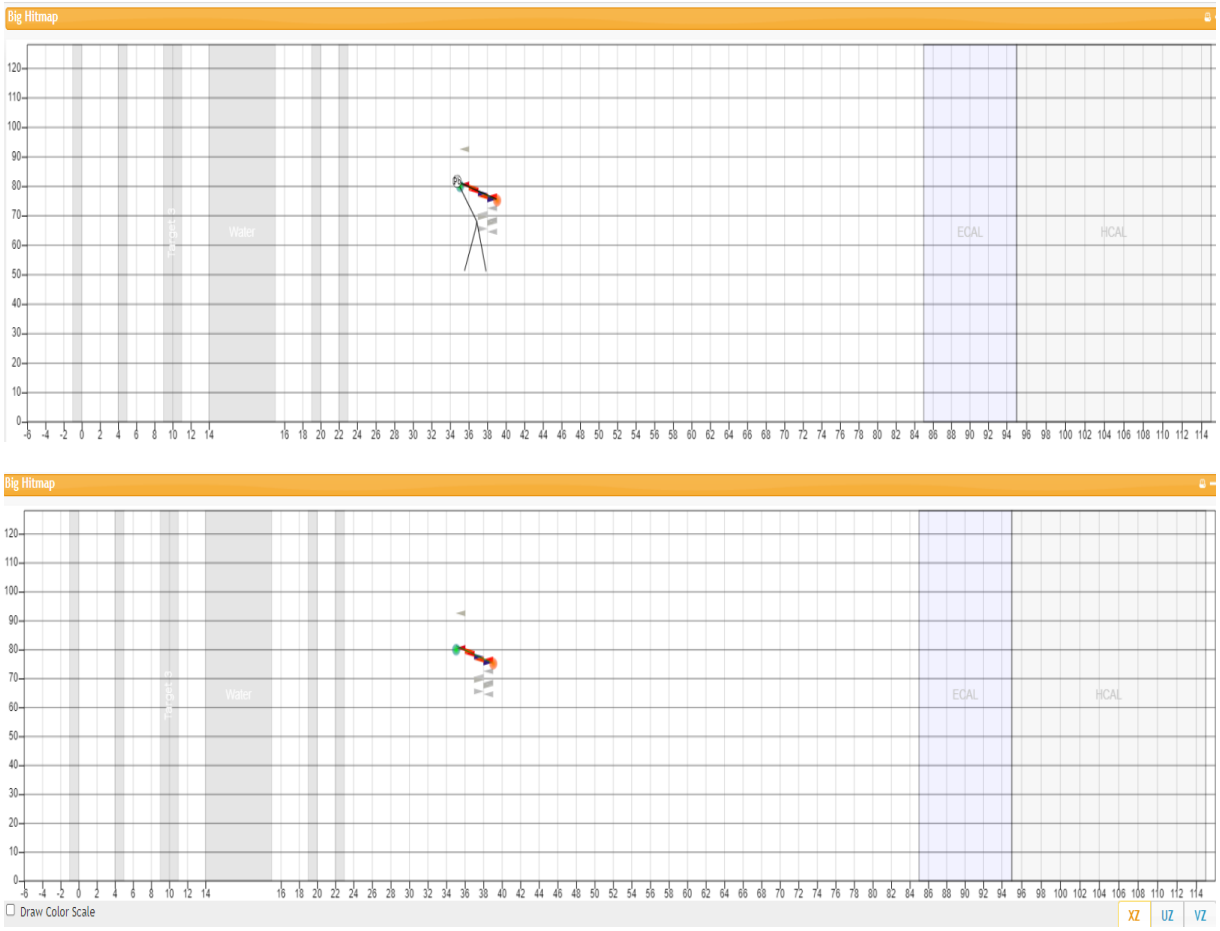

FIGURE 4.5: Both hitmaps show the same slice. Top diagram has MC on, here a 198 MeV neutron can be "seen" scattering downwards and depositing energy. The bottom diagram has the MC tracking off, here the reconstructed track of a 187MeV proton is clearly displayed

The Monte Carlo Digraph is useful for interpreting the untracked evolution of the interaction. Neutrinos and neutrons are neutral and therefore cannot be tracked inside the detector but the energy they deposit can be seen as PMT hits. Coupling the diagraph with the MC overlay, it can be seen that the neutron heads towards the outer detector and deposits a small amount of energy in the active tracker region before being stopped in the OD. The tracking information can be viewed by clicking on either the track itself, or the red or green dot. Doing so brings up a comment box that contains values associated with the tracked event as well as estimates depending on if it is a tracked proton or a tracked muon.

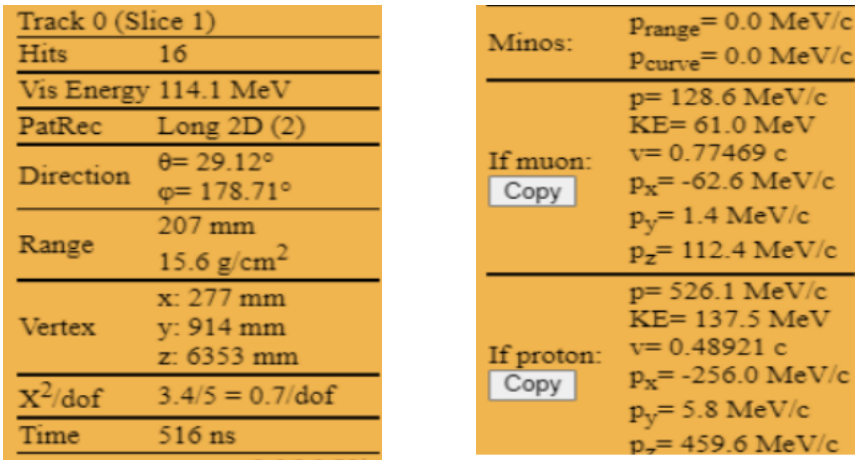

FIGURE 4.6: selecting a track shows information about the track reconstruction: visible energy (total energy of the hits associated with the track), direction w.r.t the beamline axis, initial vertex position in detector reference frame, χ^2/dof gives the reconstruction accuracy, time length of the track, particle information if the track represents a muon, particle information if it is a proton

Within the schematic, each PMT hit is represented by a small triangle meant to mimic the scintillator slices in the actual detector. Each triangle is assigned a color depending on the energy deposited; this ranges from white (no energy deposition) to dark purple (high energy deposition), so the darker the color the higher the energy signature. The simulated event displayed in the previous images shows the scattering of a neutrino off a Pb nucleus. This knocks out a proton and a neutron that then continue to interact with surrounding parts of the active tracker region. In the case of the 178 MeV proton, it contains enough energy that a well-defined track was able to be created. It can be seen depositing large amounts of energy over a short region before loosing all momentum. In the case of the 198 MeV neutron, it appears invisible within the detector (not tracked) however its particular hit signature is easily recognizable: no hits or tracked particle then a seemingly sudden large deposition of energy. This large energy deposition can be seen in the bottom outer detector region of the UZ hit map.

In order to estimate a neutron background for our data, we must go through these simulated DST files to pick out events that contain nicely tracked protons that were mostly likely hit by neutrons instead of neutrinos.

Chapter 5

Methods

The data supplied from the MinerνA collaboration is housed in ROOT files were information about interactions and hits are compiled into NTuples and stored as trees. This process is done using the formerly described GAUDI, GENIE, and GEANT4 softwares. All of the data collection had been done previously and stored for later use, so the process of obtaining and formatting the data was not part of this analysis. After externally reformatting these into workable text files that could be read by Python libraries, the data was in a usable configuration for what we wanted to investigate.

We began looking at the MC simulated rock muons since the most information about them was known. Muons are also easily tracked and viewed using the MINOS detector as well as their hits being visible in the MINERνA setup. This allow for easier verification that the developed algorithm was giving us correct information. (An explanation of the Python script analysis process will be described in further detail in a later section).

We next examined MC events in the downstream ECAL, and those simulated in the outer detector region. The hope with these files was that the simulated events could begin to give us a profile of the background level of neutron scattering events within out sample so we could later estimate a similar background in the actual data sample. Following this, we characterized MINERνA vertex events to look at interactions

specifically in the active tracker region. The simulated data samples we had available contained sets in both the FHC and RHC orientation.

These data sets were largely formatted in the same way: individual rows contained information about *one* "hit", where a hit is an energy deposit to a scintillator by a particle (these are shown well in the Arachne chapter as different colored triangles in the 2D detector schematic where colors correspond to the energy deposited). Each hit contained information about the particle's PDG (based on the MC numbering scheme), vertex position (x, y, z), momentum vector (x, y, z), energy. And some, but not all, also contained information about the run number, event number, and time. When obtained from MINERνA databases, these sets were formatted as ROOT files. ROOT being a C++ based software is incompatible with the Python script created to process the events. Reformatting them into .txt files allow me to use PANDAS dataframes to more quickly extract specific variables to confirm the profile of the dataset, and eventually to produce visualization of varying relationships of the even hits.

5.1 Dataset Characterization

5.1.1 Script Validity Testing

The first step in any data analysis, or when working with any dataset, is to confirm that the data being used is properly structured and that it, to a reasonable degree, contains accurate information. By converting the text file into a PANDAS DataFrame, we were able to investigate the dataset profile from a data science perspective to fully understand the information available to me and what I could learn from it.

The dataset was structured in a way that each line represented a "hit" and each hit was a characterization of a detected particle. Each line in the data file contain information about that hit's run number, event number, line number, index number, ipdg (Monte Carlo particle numbering scheme), 3-momentum, total energy, spacial coordinate, and time. The first hurdle, came in actually loading the text file into the Python

workspace. This problem originated from the fact that many of the data lines in the file had missing information and needed to be filtered out since they were unusable.

After removing the hits with missing information, I began investigating incoming beam based on FHC and RHC data.

Particles	**PDG Scheme**
proton	2212
neutron	2112
e^-	11
ν_e	12
μ^-	13
ν_μ	14
τ^-	15
ν_τ	16

TABLE 5.1: MC pdg numbering scheme.

5.1.2 Data Filtering

After characterizing the data and determining that the PANDAS was the best python package to use, I began work on calculating the neutron background.

As stated in Chapter 4, the detector consists of an inner detector and outer detector which is preceded by rock. As the beamline passed through that rock, it has the potential to interact with the rock and produce muons. Similarly, there is the potential for muons produced in outer detector events to enter the inner detector and create hits. This causes an issue since all neutral particles assigned to an event are labeled "neutron" however many will be neutrinos. The goal is to estimate how many of the events are actually neutrons, no neutrinos, and create a background that can be subtracted from the total dataset. In theory, leaving behind *only* neutrino events. This could be done using simulated events, before applying it to the real dataset.

When attempting to calculate the neutron background, I found events that seemed to contain upwards of twenty muons produced in a single interaction, which is statistically unfavorable. After reviewing the data, I realized that during the data collection process separate runs re-used event numbers thus making it a non-unique value. It was

necessary in having completely unique ways to group the data into separate events. By altering the event number using run number and line number, I was able to create completely unique identifiers for each actual event.

The first objective was to analyze the distribution of muon count vs neutron count in each event. This is an important step in distinguishing between neutron and neutrino events since more "chaotic" scatterings favor a neutron hit over a neutrino one. The first set of neutron data came from the rock simulation, as the beam passed through the 250m of rock, and as externally generated particles interact with the inner detector, there will be an influx of muons not generated by neutrino interactions. Looking at the distribution of neutrons produced at the same time as muons gives us an idea of the total neutron distribution. However, some of these could possibly be neutrinos.

After making all the event numbers properly unique, I still found that there were events containing two and even three muons. However, those were so few in frequency, and therefore statistically unlikely, I felt confident discarding those and focusing only on the events containing zero or one muon.

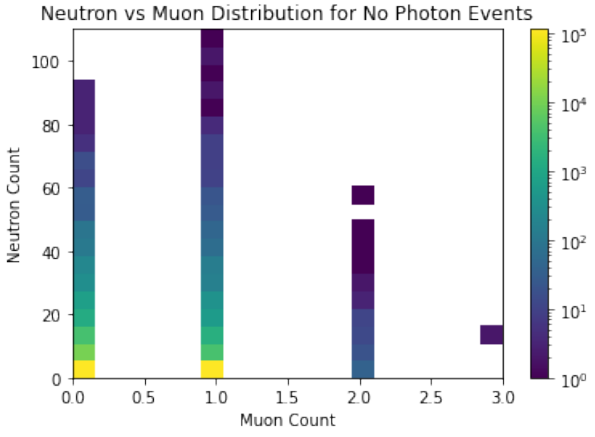

FIGURE 5.1: Distribution of neutrons vs muons from rock simulation

After cutting down to look at only events with zero or one muon I was still left with over ninety-nine percent of our original data points.

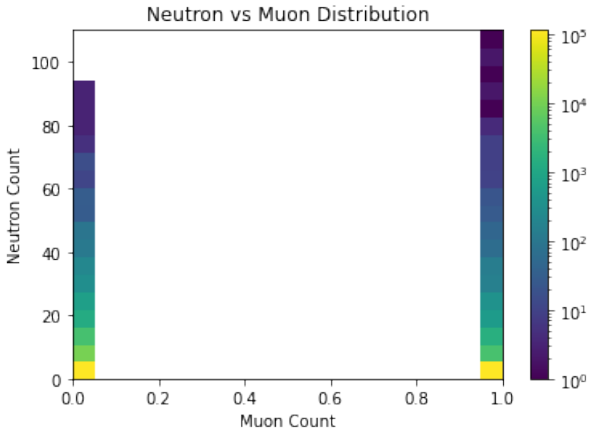

FIGURE 5.2: Rock generated events with only zero or one muon

5.1.3 Energy Distribution

For my specific approach to finding the differential cross-section of neutral current scattering is dependent on the relationship between scattering angle and incident energy. In order to achieve this, further data manipulation to get the correct distribution. First, the energy information in the hits contains the total energy of the final state particles. I wanted the distribution with respect to kinetic energy (T) instead of total energy. To find this I used the below formula:

$$E_{total} = mc^2 + T \tag{5.1}$$

Here, the rest mass energy (RME) (mc^2) is completely dependent on the type of particle. So subtracting the RME from the total energy will result in the kinetic energy of the particle. Similarly, the incident angle can be found from the particle momentum. The momentum and coordinate information given in the data set is respect to the x-y-z coordinates defined in the earlier sections. However, I want the angle with respect to the beamline, so a coordinate transfer is necessary. Below is a schematic that visually represents the axis transformation from the laboratory frame (unprimed) to the beamline frame (primed).

This can be achieved using the standard coordinate transformation tensors:

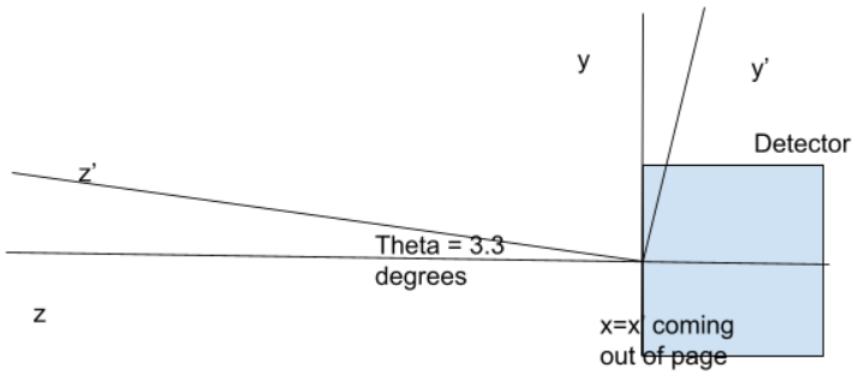

FIGURE 5.3: Axis Transformation Visual

$$R_x(\theta) = \begin{pmatrix} 1 & 0 & 0 \\ 0 & cos(\theta) & -sin(\theta) \\ 0 & sin(\theta) & cos(\theta) \end{pmatrix} \tag{5.2}$$

$$R_y(\theta) = \begin{pmatrix} cos(\theta) & 0 & sin(\theta) \\ 0 & 1 & 0 \\ -sin(\theta) & 0 & cos(\theta) \end{pmatrix} \tag{5.3}$$

$$R_z(\theta) = \begin{pmatrix} cos(\theta) & -sin(\theta) & 0 \\ sin(\theta) & cos(\theta) & 0 \\ 0 & 0 & 1 \end{pmatrix} \tag{5.4}$$

5.2 Selecting Eligible Events

The goal is to computationally select events that fit the profile of neutrino-proton scattering and ones that are mostly likely neutron-proton scattering. If the datasets were smaller, this would be done by hand through simply looking at each event and determining possibly usable ones. However, the full collection of data contains tens of millions of events and is unmanageable to do by hand. In order to automate the process, we need

to establish characteristics that separate interesting events from ones we do not need. Some parameters of interest include:

- *n_tracks*: number of tracks per event
- *n_rawhits*: number of raw hits per event
- *n_slices*: number of slices per event
- *n_idhits*: number of inner detector hits
- *n_odhits*: number of outer detector hits
- *hit_time_slice*: recorded time slice
- *trk_time_slice*: recorded time slice for reco track
- *trk_vis_energy*: visible energy of reco track
- *trk_theta*: angle of track w.r.t beamline
- *trk_chi2perDof*: goodness of reco track fit
- *trk_phi*: xy distribution of hits
- *trk_nodes*: distinguishes shorter vs longer tracks

The first level of distinction comes from data files containing cuts with one defined track contained within the active tracker region. Looking for files with $n\_tracks = 1$ will quickly filter out data that is not useful. Next, we have to differentiate between protons that were scattered by neutrons versus neutrinos. This can be done by looking at the frequency of inner and outer detector hits: outer detector hits indicate that it was probably *not* a clean neutrino interaction in the inner detector. In addition to this, shorter nicely modelled tracks are more likely neutrino scattering events.

Chapter 6

Results and Discussion

We obtained a distribution of scattering angle versus incident energy that was consistent with what was physically expected. Within scattering experiments, scattering angle is proportional to the inverse cotangent of kinetic energy: when graphed this creates the exponential decay-like diagram that is shown below. It was also a consistent distribution across the board: the higher the energy the smaller the scattering angle.

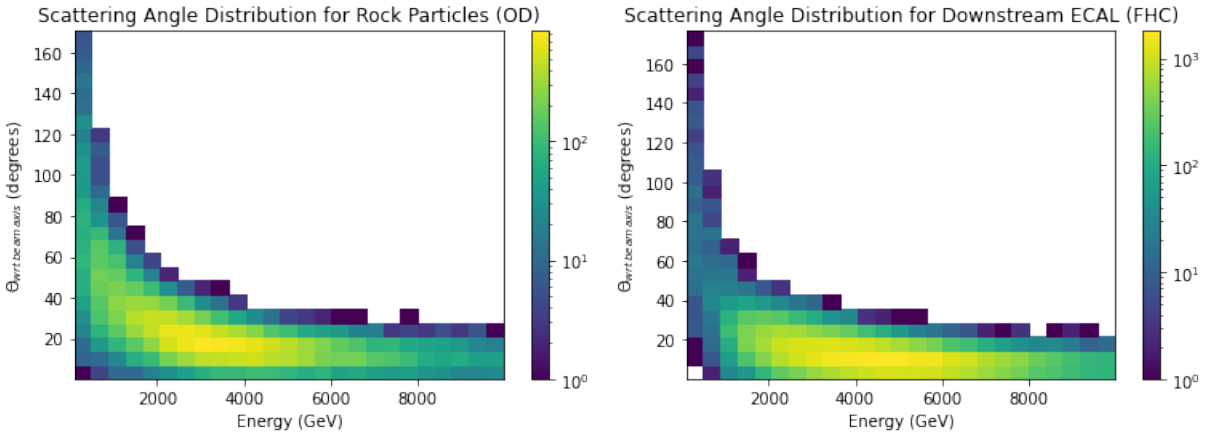

FIGURE 6.1: Dataset validity started by confirming that the scattering angle-kinetic energy relationship for the particles followed $\theta \propto \cot^{-1}(T)$

The overall goal when characterizing scattering interactions is to find the total cross-section of the process. Broken down, scattering cross-sections give the probability that the specific scattering interaction will take place based on a certain variable: in

particle physics this probability is often with respect to scattering angle or incident particle energy.

The full expression for experimentally finding the total neutrino-proton scattering cross-section is shown below:

$$\sigma_i = \beta \frac{\sum_j U_{ij} \left(N_j^{DATA} - N_j^{BKGD} \right)}{\epsilon_i \phi_i T} \tag{6.1}$$

σ represents the cross-section based on the summation of data from reconstructed (j) events: where β is the material correction factor, U_{ij} is the unfolding matrix, ϵ_i is the efficiency, ϕ_i is the flux per bin, T is the number of nuclei, and the two N are the number of data events versus the number of predicted background events. The criteria for selecting data and background events using certain ROOT tree parameters is detailed in section 5.2.

Within the constraints of this research project, the goal was to identify parameters for selecting eligible NC elastic neutrino-proton events from the raw data file. This would eventually allow for the calculation of N_j^{DATA} and N_j^{BKGD}. This was done by characterizing the datasets for the MC simulated events: rock muons, DSE, etc, to create a python script that would first verify properly formatted data, sift out any data lines that did not contain adequate information, plot angle vs energy distribution to confirm basic physics of the interaction, and finally, identify if the scattering process was done by a neutrino or a neutron.Using MC events to do this was crucial since the truth tables of the interactions were already known: we would know when the incident particle was a neutrino, neutron, or even some other elementary particle. Once we were able to access the raw data from the MINERνA collaboration we already had algorithms created to properly format and process that large datasets.

We ultimately ran into roadblocks that prevented the actual selection of events within the time frame of the thesis. However, with the algorithm created, a future individual would be set up for success in moving forward with the raw data. Additionally,

in the future, to calculate the full cross-section the unfolding matrix and the efficiency would need to be estimated. The flux is a quantity calculated independently through MINERνA instrumentation and is readily available to the researcher. The time available for this thesis and with the available computing power made it unreasonable to attempt estimating these other cross-section parameters.

Now, it is useful to document in detail the challenges faced during the research and how they were addressed; in case it may be helpful for any individual who is interested in picking up with project in the future.

Accessing MINERνA files and database:

All data files are housed in Fermi Labs protected databases, so without official access they are unobtainable. Remote access to files and MAT download can be done by another individual in the collaboration with proper authorization. The same thing can be done for Arachne access. Extracting the data was done completely by my advisor before being uploaded into a shared Google Drive for easy access.

MAT and ROOT installation:

Most of the collaboration uses a framework called MAT to access, view, analysis, and eventually plot the data. Depending on the computer type and operating system installing this may not be possible. The collaboration has step-by-step instructions on the installation of both MAT and ROOT. However, on my Windows 11 HP laptop ROOT was functional and MAT was not. This prompted using Google Colab for file manipulation and plotting instead of using the C++ algorithms in MAT. It was still possible to view histograms of the .root data files but not analyze them in the desired fashion. This may not be an issue for a future individual that has access to the installation directly from the collaboration but still something to look out for.

Files with Non-unique Run Numbers:

Only MC simulated data files have the potential to have this problem because of the way they are formatted. Each line of the data represents a particle hit within the

detector and contains information about the particle PDG, vertex, momentum, energy, time slice, and event number. Ideally, each event in a single data file would have a unique number. However, we discovered that data collected at different run times would reuse event numbers so particles would be grouped together into one event that actually happen at two separate times. To alleviate this issue, a combination of event number a line number was created to problem group hits in the same event, this way we could look at energies, momentum, and angles for events separately. As stated, this was not an issue with *all* of the data sets so part of the constructed python script checks for this issue.

Not all MINERνA files "online":

All MINERνA data is stored on tape and is accessible to be downloaded. However, for data usage reasons it is not kept "online" at all times and requests for specific data sets must be made for it to be brought "online". Since the MINERνA project is nearing the end of its days (no new data being taken), other active experiments are given priority for their data. This can bring analysis to a standstill if there is no space online for more files: a request could sit for weeks or even longer.

Data file size eats up too much RAM:

Using Google Colab was incredibly useful so that my advisor could see my work in real time. However, only a small amount of RAM is allowed for the free account. The data sets, even formatted as .txt files, contained multiple GBytes of information so with normal approaches the Colab server would crash. This problem was addressed by breaking up data sets into smaller chunks before loading into the server, using PANDAS dataframes with the file loaded using *loadcsv* allowing it to load in one line at a time, and by purchasing more RAM. Of course the last option is if nothing else works to solve the problem. If the research is funded that cost could easily be covered. I simply footed the bill because the extra RAM was crucial to completing the work.

Improperly identified particles in the raw data and possible CC bias:

Our initial approach to separating out neutrino-proton and neutron-proton scattering in the raw data was to pick out events containing slices with one tracked proton. One nice track in the slice indicated there was mostly likely a decent neutrino interaction that hit a proton with high energy. We found however that the only data returned using this condition also contained a muon in the slice that had the same vertex position as the proton: it was returning *only* charged current events. It may be that since MINERνA has been primarily studying CC events, the reconstruction and tracking algorithms that were developed are biased towards that type of interaction. This led us to investigate other ways to identify neutrino events. Furthermore we noticed that within events containing both protons and muons, often times the energy per hit associated with the muons varied wildly. When doing a visible energy per node analysis of two different particles both identified as muons, one had a low ratio of $\sim$ 3MeV/node (probably a rock muon) but the other had $\sim$ 11MeV/node. The latter is more characteristic of a proton than a muon so perhaps particles are being incorrectly tracked as well. This prompted an investigation of the full data set and we found that most muons followed the 3 MeV/node trend but there was also a significant number of "high-energy" muons that sat under the proton energy peak, leading use to believe they are actually protons. This could possibly explain way we were not able to computationally extract the events we were looking for.

The Figure 6.2 shows a distribution of visible energy per node for the raw data set lines containing one tracked proton. As can be seen, there are a large number of "high energy" muons that more closely fit the profile of a 5MeV proton, meaning they may have been mislabelled within the identification algorithm.

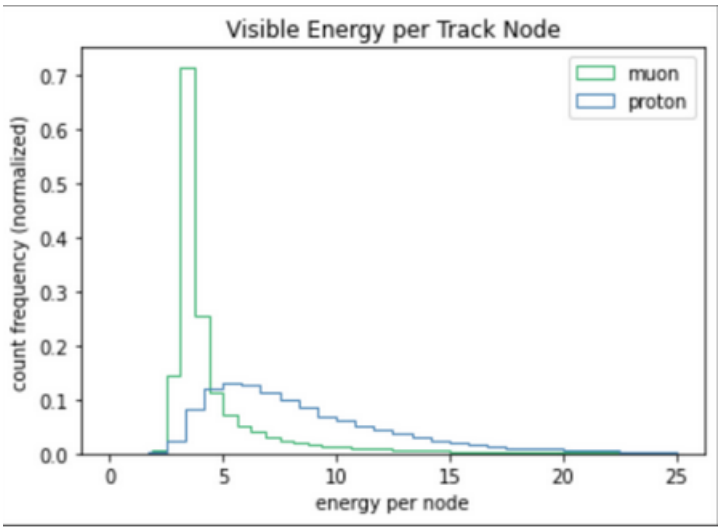

FIGURE 6.2: Distribution of particle's visible energy (MeV) per node for raw data files, separated by muon or proton identification

---

Based on the mixing matrix calculated in Appendix C, and the basic formula for two-body scattering cross section, we obtain a a range of $\sigma \approx 10^{-42}$ cm^2 to 10^{-42} cm^2 for incident neutrino energies of 100MeV to 10GeV. This is comparable to the values found experimentally and recorded in the Particle Data Group.

Finding a total cross-section neutrino-proton elastic scattering in the mid-energy range would be incredibly beneficial for upcoming neutrino experiments such as DUNE in establishing calibration data for their detectors. Hopefully, with these insights about the data and the process other individuals can pick up where the project was left off with relative ease.

Chapter 7

Conclusion

Within the time constraints of this thesis, we were able identify a set of parameters for finding neutrino-proton scattering events within the data collected by the MINERνA experiment. Those events were characterized using a Python algorithm detailed in Appendix D. We selected these parameters with the goal of eventually being able to numerically characterize events as ones of interest, so that the number of data events and number of estimated background events could be calculated in the future: one component in estimating the full cross-section expression for these interactions. Moving forward, efficiency and the unfolding matrix must be estimated, and the flux pr bin must be retrieved from the collaboration to find a final estimate of the total cross-section.

In order to accomplish these future goals it would be more beneficial to approach the process of data analysis using MINERνA's already developed MAT framework that is equipped to utilize the files in their raw format and has all the necessary parameters self-contained. Using Python DataFrames for the neutron background analysis, though better for visualizing the information, was cumbersome when it came to applying the outcomes later: the process of converting ROOT files to .txt format to then filter and plot proved computationally memory intensive in addition to being time consuming. It would be better to keep the data in its original file format in the future and attempt to perform

a similar analysis using ROOT plotting tools. Other challenges a future individual may face , and their solutions, have been detailed in the Results and Discussion chapter.

Appendix A

Fundamentals of Feynman Diagram Calculations

When starting the journey of understanding neutrino interactions with matter, the first step is to understand Feynman dynamics at its most basic level. Feynman diagrams are the visual representation of processes that can be as simple as a single elastic collision, or as complicated as neutrino deep inelastic scattering. In breaking down the scattering process that applies to this specific thesis, the following Feynman diagrams have the potential to provide a full description.

To begin the process of finding an expression for the differential cross-section,it is essential to establish all possible variations of the desired interaction. In this case, the only two possible orientations for neutral current scattering are shown in Figure A.1.

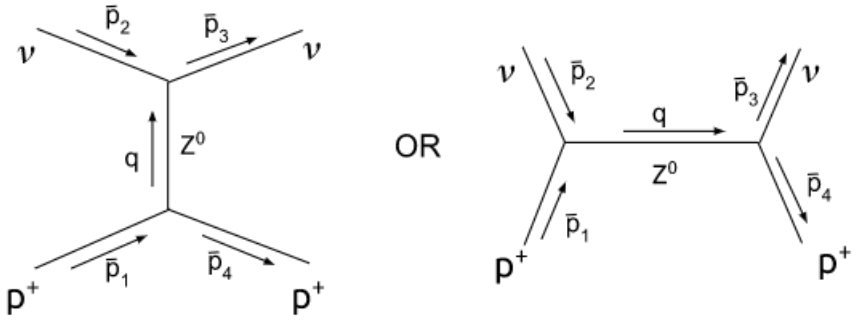

FIGURE A.1: Possible Feynman diagrams for ν-p^+ scattering

For simple scattering, not yet adding QED or QCD, the next is to find the mixing matrix $\mathcal{M}$ for the simple elastic scattering of the neutrino and proton view the Z boson as the mediator particle. It is easiest to approach each diagram separately at the beginning.

Let's label the left interaction as Diagram A and the right as Diagram B. The basic steps for calculating the dynamics in a Feynman diagram are to:

1. label all the incoming and outgoing momenta with $\bar{p_i}$, and any internal momenta with $\bar{q_j}$
2. assign a -ig and $(2\pi)^4\delta^2(k_1 + k_2 + ... + k_i)$ to each vertex; when creating the delta function, k_i represents the 4-momentum of all particles at that specific vertex: given a positive sign if the particle is incoming and negative if outgoing
3. for each *internal* line assign a $i/(q_j^2 - m_j^2c^2)$, where m_j is the mass of the internal particle and q_j is its 4-momentum. Also assign each internal line a $(2\pi)^{-4}d^4q_j$
4. integrate over the internal momenta until the final expression is only in terms of $\bar{p_i}$
5. cross out any remaining delta functions and multiply by $i(2\pi)^{-4}$. The remaining expression is $\mathcal{M}$, the mixing matrix

. In its most basic form the total cross-section takes the form:

$$\sigma = \frac{s\hbar^2}{4\sqrt{(p_1 \cdot p_2)^2 - (m_1 m_2 c^2)^2}} \int |\mathcal{M}|^2 (2\pi)^4 \delta^4(p_1 + p_2 - p_3 ... - p_n) \times \prod_{j=3}^{n} \frac{1}{2\sqrt{\bar{p_j}^2 + m_j^2 c^2}} \frac{d^3\bar{p_j}}{(2\pi)^3} \quad \text{(A.1)}$$

DIAGRAM A:

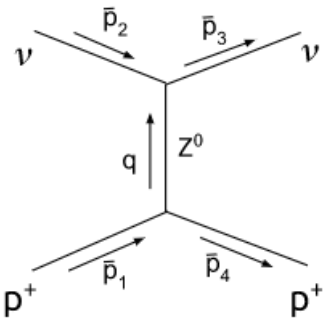

Step 1: the diagram to the right already has all incoming, outgoing, and internal momenta labelled with unique indices.

Step 2: there are two vertices, so there will be two -ig 's. The top vertex vertex is given $(2\pi)^4\delta^4(\bar{p_2}+\bar{q}-\bar{p_3})$, the bottom has $(2\pi)^4\delta^4(\bar{p_1}-\bar{p_4}-\bar{q})$

Step 3: for the one internal line there is $i/(q^2-m_Z^2c^2)$ and $(2\pi)^{-4}d^4q$

Step 4: This gives the integral:

$$-i(2\pi)^4\mathcal{M}_{\mathcal{A}} = \int(-ig)^2[(2\pi)^4]^2\frac{i}{q^2-m_Z^2c^2}\delta^4(\bar{p_2}+\bar{q}-\bar{p_3})\delta^4(\bar{p_1}-\bar{p_4}-\bar{q})\frac{1}{(2\pi)^4}d^4q$$

The goal is to allow the delta functions including internal momentum to go to one. To do this let:

$$q = \bar{p_3}-\bar{p_2}$$

The R.H.S of the equation then becomes after integrating over q:

$$-ig^2(2\pi)^4\frac{1}{(\bar{p_3}-\bar{p_2})^2-m_Z^2c^2}\delta^4(\bar{p_1}+\bar{p_2}-\bar{p_3}-\bar{p_4})$$

Step 5: After crossing out $\delta^4(\bar{p_1}+\bar{p_2}-\bar{p_3}-\bar{p_4})$ and multiplying by $i(2\pi)^{-4}$ the final expression for the mixing matrix of this scattering event is:

$$\mathcal{M}_{\mathcal{A}} = \frac{g^2}{(\bar{p_3}-\bar{p_2})^2-m_Z^2c^2}$$

DIAGRAM B:

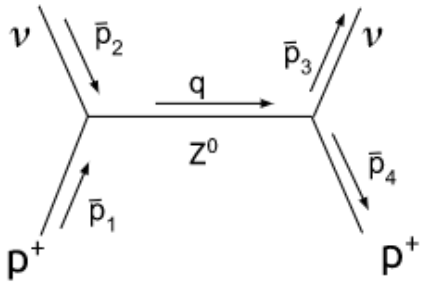

The process for finding $\mathcal{M}_{\mathcal{B}}$ is identical to finding $\mathcal{M}_{\mathcal{A}}$ so following the same steps as for Diagram A.

From Step 2 there is $(-ig)^2$, $(2\pi)^8$, $\delta^4(\bar{p_1} + \bar{p_2} - \bar{q})$, and $\delta^4(\bar{q} - \bar{p_3} - \bar{p_4})$. Step 3 gives the same results as in Diagram A since the mediator particle and process are identical.

Step 4 gives the following equation:

$$-i(2\pi)^4\mathcal{M}_{\mathcal{B}} = \int (-ig)^2[(2\pi)^4]^2 \frac{i}{q^2 - m_Z^2c^2}\delta^4(\bar{p_1}+\bar{p_2}-\bar{q})\delta^4(\bar{q}-\bar{p_3}-\bar{p_4})\frac{1}{(2\pi)^4}d^4q$$

The delta function that needs to be set to one is $\delta^4(\bar{q} - \bar{p_3} - \bar{p_4})$. That is done by setting $q = \bar{p_3} + \bar{p_4}$. Integrating over $\bar{q}$ and multiplying by $i(2\pi)^{-4}$ gives:

$$\mathcal{M}_{\mathcal{B}} = \frac{g^2}{(\bar{p_3} + \bar{p_4})^2 - m_Z^2c^2}$$

The expression for the *total* mixing matrix of the neutral scattering reaction is the simple addition of the the mixing matrices for all the possible variation of the interaction.

$$\mathcal{M}_{total} = \mathcal{M}_{\mathcal{A}} + \mathcal{M}_{\mathcal{B}} = g^2\left(\frac{1}{(\bar{p_3} - \bar{p_2})^2 - m_Z^2c^2} + \frac{1}{(\bar{p_3} + \bar{p_4})^2 - m_Z^2c^2}\right) \tag{A.2}$$

As previously stated, this expression for $\mathcal{M}$ is only for the scattering of two particles assuming a simple interaction and not incorporating the intricacies of QED or QCD.

The next steps to finding the differential cross-section is to breaking down $\mathcal{M}_{total}$ into measurable quantities in the lab frame of reference. The goal is to obtain the cross-section in terms of *only* these quantities.

The scattering process from this perspective takes the form:

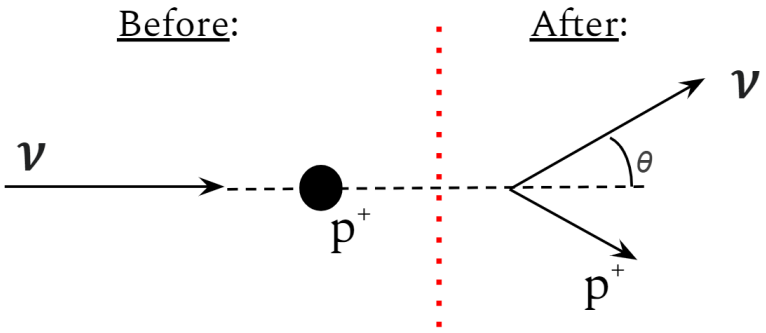

FIGURE A.2: ν-p^+ scattering in the lab reference frame

Using the formalism from the before calculations:

$$\begin{aligned} p_1 = p_p &= (E_{p,i}, \vec{p}_{p,i}) = (m_p c^2, 0) \\ p_2 = p_{\nu,i} &= (E_{\nu,i}, \vec{p}_{\nu,i}) = (\frac{E_2}{c}, \vec{p}_2) \\ p_3 = p_{\nu,f} &= (E_{\nu,f}, \vec{p}_{\nu,f}) = (\frac{E_3}{c}, \vec{p}_3) \\ p_4 = p_{p,f} &= (E_{p,f}, \vec{p}_{p,f}) = (\frac{E_4}{c}, \vec{p}_4) \end{aligned} \tag{A.3}$$

The next goal is to find the 4-momentum components of $\mathcal{M}$ in terms of particle energy, and 3-momenta.

$$(p_3 - p_2) = \begin{bmatrix} E_3/c \\ \vec{p}_3 \end{bmatrix} - \begin{bmatrix} E_2/c \\ \vec{p}_2 \end{bmatrix} = \left(\frac{E_3 - E_2}{c}, \vec{p}_3 - \vec{p}_2 \right)$$

Let's call $p_a = (p_3 - p_2)$ and $\vec{p}_a = (\vec{p}_3 - \vec{p}_2)$, using the mathematical and physical identities:

$$(p_a)^2 = \left(\frac{E_a}{c} \right)^2 - (\vec{p}_a)^2 \tag{A.4}$$

$$(\vec{a} \pm \vec{b})^2 = |\vec{a}|^2 + |\vec{b}|^2 \pm 2\vec{a} \cdot \vec{b} \tag{A.5}$$

$$\vec{a} \cdot \vec{b} = |\vec{a}||\vec{b}| cos\theta \tag{A.6}$$

Applying Equation A.4 and then Equation A.5:

$$\begin{aligned}(p_3 - p_2)^2 &= \left(\frac{E_3 - E_2}{c}\right)^2 - (\vec{p}_3 - \vec{p}_2)^2 \\ &= \left(\frac{E_3 - E_2}{c}\right)^2 - |\vec{p}_3|^2 - |\vec{p}_2|^2 + 2\vec{p}_3 \cdot \vec{p}_2 \\ &= \left(\frac{E_3 - E_2}{c}\right)^2 - |\vec{p}_3|^2 - |\vec{p}_2|^2 + 2|\vec{p}_2||\vec{p}_3| cos\theta\end{aligned}$$

Doing the same process for $(p_3 + p_4)$ gives:

$$(p_3 + p_4)^2 = \left(\frac{E_3 + E_4}{c}\right)^2 - |\vec{p}_3|^2 - |\vec{p}_4|^2 - 2|\vec{p}_3||\vec{p}_4| cos\theta$$

This transforms Equation A.2 into

$$\begin{aligned}\mathcal{M}_{total} = g^2 \Bigg(&\frac{1}{\left(\frac{E_{\nu,f} - E_{\nu,i}}{c}\right)^2 - |\vec{p}_{\nu,f}|^2 - |\vec{p}_{\nu,i}|^2 + 2|\vec{p}_{\nu,i}||\vec{p}_{\nu,f}| cos\theta - m_Z^2 c^2} \\ &+ \frac{1}{\left(\frac{E_{\nu,f} + E_{p,f}}{c}\right)^2 - |\vec{p}_{\nu,f}|^2 - |\vec{p}_{p,f}|^2 - 2|\vec{p}_{\nu,f}||\vec{p}_{p,f}| cos\theta - m_Z^2 c^2} \Bigg)\end{aligned} \tag{A.7}$$

From Equation A.1, the square root in the denominator can be considerably simplified:

$$\begin{aligned}(p_1 \cdot p_2)^2 &= (m_1 c \times \frac{E_2}{c} + \vec{p}_2 \times 0)^2 \\ &= m_1^2 E_2^2 = m_p^2 E_\nu^2\end{aligned}$$

$$\begin{aligned}\mu &= \sqrt{(p_1 \cdot p_2)^2 - (m_1 m_2 c^2)^2} \\ &= (m_1^2 E_2^2 - m_1^2 m_2^2 c^4)^{\frac{1}{2}} \\ &= \left[m_1^2 c^2 \left(\left(\frac{E_2}{c}\right)^2 - m_2^2 c^2\right)\right]^{\frac{1}{2}} \\ &= m_1 c |\vec{p}_2| = m_1 c |\vec{p}_{\nu,i}|\end{aligned}$$

This simplification transforms Equation A.1 into

$$\sigma = \frac{s\hbar^2}{4|\vec{p}_2|m_p c}\int |\mathcal{M}|^2(2\pi)^4\delta^4(p_1 + p_2 - p_3 - p_4)\prod_{j=3}^{n}\frac{1}{2\sqrt{\bar{p_j}^2 + m_j^2c^2}}\frac{d^3\bar{p_j}}{(2\pi)^3} \quad \text{(A.8)}$$

Calculating the product operator within the integrand

$$\begin{aligned}\prod_{j=3}^{4}\frac{1}{2\sqrt{\bar{p_j}^2 + m_j^2c^2}}\frac{d^3\bar{p_j}}{(2\pi)^3} &= \left(\frac{1}{2\sqrt{\vec{p}_3^2 + m_3^2c^2}}\frac{d^3\vec{p}_3}{(2\pi)^3}\right)\left(\frac{1}{2\sqrt{\vec{p}_4^2 + m_4^2c^2}}\frac{d^3\vec{p}_4}{(2\pi)^3}\right)\\ &= \frac{1}{4(2\pi)^6}\left(\frac{d^3\vec{p}_3}{\sqrt{\vec{p}_3^2 + m_3^2c^2}}\right)\left(\frac{d^3\vec{p}_4}{\sqrt{\vec{p}_4^2 + m_4^2c^2}}\right)\end{aligned}$$

Plugging this into Equation A.8

$$\begin{aligned}\sigma = \frac{s\hbar^2}{4|\vec{p}_2|m_p c}\left(\frac{1}{4\pi^2}\right)\int |\mathcal{M}|^2\delta^4(p_1 + p_2 - p_3 - p_4)\\ \times\left(\frac{d^3\vec{p}_3 d^3\vec{p}_4}{\sqrt{\vec{p}_3^2 + m_3^2c^2}\sqrt{\vec{p}_4^2 + m_4^2c^2}}\right) \quad \text{(A.9)}\end{aligned}$$

Now using the conditions that

$$\vec{p}_2 = 0$$
$$p_j^0 = \sqrt{\vec{p}_j^2 - m_j c}$$

p_j^0 are the rest mass energies of the respective particles

$$p_1^0 = \frac{E_1}{c} \qquad p_3^0 = |\vec{p}_3|$$
$$p_2^0 = \frac{E_2}{c} \qquad p_4^0 = |\vec{p}_4|$$

This is useful in simplifying Equation A.9

$$\begin{aligned}\delta^2(p_1 + p_2 - p_3 - p_4) &= \delta(p_1^0 + p_2^0 - p_3^0 - p_4^0)\delta^3(\vec{p_1} + \vec{p_2} - \vec{p_3} - \vec{p_4})\\ &= \delta(\frac{E_1 + E_2}{c} - |\vec{p}_3| - |\vec{p}_4|)\delta^3(\vec{p_1} - \vec{p_3} - \vec{p_4})\end{aligned}$$

Applying the same method for calculating the delta function, let $\vec{p}_4 = \vec{p}_1 - \vec{p}_3$. This will give the differential cross section w.r.t the solid angle Ω

$$\frac{d\sigma}{d\Omega} = \left(\frac{\hbar}{8\pi}\right)^2 \frac{s}{|\vec{p}_2|m_p c} \int \frac{|\mathcal{M}|^2 \delta(\frac{E_1+E_2}{c} - \sqrt{\vec{p}_3^2 + m_3^2c^2} - \sqrt{(\vec{p}_1 - \vec{p}_3)^2 + m_4^2c^2})}{\sqrt{\vec{p}_3^2 + m_3^2c^2} - \sqrt{(\vec{p}_1 - \vec{p}_3)^2 + m_4^2c^2}} |\vec{p}_3|^2 d\vec{p}_3 \tag{A.10}$$

It will be easier to integrate over $\vec{p}_3$ by letting $r \equiv |\vec{p}_3|$. So Equation A.10 becomes

$$\frac{d\sigma}{d\Omega} = \left(\frac{\hbar}{8\pi}\right)^2 \frac{s}{|\vec{p}_2|m_p c} \int \frac{|\mathcal{M}|^2 \delta(\frac{E_1+E_2}{c} - (\sqrt{r^2 + m_3^2c^2} - \sqrt{r^2 + 2r|\vec{p}_1|cos\theta + |\vec{p}_1|^2 + m_4^2c^2})}{\sqrt{r^2 + m_3^2c^2} - \sqrt{r^2 - 2r|\vec{p}_1|cos\theta + |\vec{p}_1|^2 + m_4^2c^2}} \times r^2 dr \tag{A.11}$$

Also let $z \equiv \sqrt{r^2 + m_3^2c^2} - \sqrt{r^2 + 2r|\vec{p}_1|cos\theta + |\vec{p}_1|^2 + m_4^2c^2}$. Then

$$\frac{dz}{dr} = \frac{rz - |\vec{p}_1|cos\theta\sqrt{r^2 + m_3^2c^2}}{\sqrt{r^2 + m_3^2c^2} - \sqrt{r^2 - 2r|\vec{p}_1|cos\theta + |\vec{p}_1|^2 + m_4^2c^2}}$$

This transforms Equation A.11 into

$$\frac{d\sigma}{d\Omega} = \left(\frac{\hbar}{8\pi}\right)^2 \frac{s}{|\vec{p}_2|m_p c} \int |\mathcal{M}|^2 \frac{\delta\left(\frac{E_1+E_2}{c} - z\right) r^2}{|rz - |\vec{p}_1|cos\theta\sqrt{r^2 + m_3^2c^2}|} dz \tag{A.12}$$

Once again, to get right of the delta function, set $z = (E_1 + E_2)/c$. Leaving

$$\begin{aligned} \frac{d\sigma}{d\Omega} &= \left(\frac{\hbar}{8\pi}\right)^2 \frac{s}{|\vec{p}_2|m_p c} |\mathcal{M}|^2 \frac{r^2}{|r\left(\frac{E_1+E_2}{c}\right) - |\vec{p}_1|cos\theta\sqrt{r^2 + m_3^2c^2}|} \\ &= \left(\frac{\hbar}{8\pi}\right)^2 \frac{s}{|\vec{p}_2|m_p c} |\mathcal{M}|^2 \frac{|\vec{p}_3|^2}{||\vec{p}_3|\left(\frac{E_1+E_2}{c}\right) - |\vec{p}_1|cos\theta\frac{E_3}{c}|} \\ &= \left(\frac{\hbar}{8\pi}\right)^2 \frac{s}{|\vec{p}_2|m_p} |\mathcal{M}|^2 \frac{|\vec{p}_3|^2}{|\vec{p}_3|(E_1 + E_2) - E_3|\vec{p}_1|cos\theta} \end{aligned} \tag{A.13}$$

Appendix B

QED and QCD in Feynman Dynamics

B.1 Quantum Electrodynamics

The basis of the QED application to Feynman calculus rests on the mathematics used by Dirac to develop his solution to the wave equation involving charged particles. It is necessary to apply this since the incorporation of spin to Feynman calculus is complicated by the spin-$\frac{1}{2}$ of quarks and leptons. Dirac's goal was to find a solution to the wave equation that was consistent with the relativistic energy-momentum formula but that kept time to the first order. This created two first-order equations that could be applied:

$$(p^0 - mc) = 0 \qquad (p^0 + mc) = 0$$

However, this solution was not applicable when all orders of p^μ were considered. Dirac's solution to *this* problem was to establish coefficients β and γ to solve:

$$(p^\mu p_\mu - m^2c^2) = (\beta^k p_k + mc)(\gamma^\lambda p_\lambda - mc) \tag{B.1}$$

where γ^λ is a set of matrices containing all solutions.

Need:

$$\{\gamma^\mu, \gamma^\nu\} = 2g^{\mu\nu} \tag{B.2}$$

$$\{A, B\} = AB + BA \tag{B.3}$$

$$g = \begin{bmatrix} 1 & 0 & 0 & 0 \\ 0 & -1 & 0 & 0 \\ 0 & 0 & -1 & 0 \\ 0 & 0 & 0 & -1 \end{bmatrix} \tag{B.4}$$

g called Minkowski metric.

Bjorken and Drell convention gives:

$$\gamma^0 = \begin{pmatrix} 1 & 0 \\ 0 & -1 \end{pmatrix} \tag{B.5}$$

$$\gamma^i = \begin{pmatrix} 0 & \sigma^i \\ -\sigma^i & 0 \end{pmatrix} \tag{B.6}$$

Note σ^i where i=1,2,3 and are called the Pauli spin matrices

$$\sigma^1 = \sigma_x = \begin{pmatrix} 0 & 1 \\ 1 & 0 \end{pmatrix} \tag{B.7}$$

$$\sigma^2 = \sigma_y = \begin{pmatrix} 0 & -i \\ i & 0 \end{pmatrix} \tag{B.8}$$

$$\sigma^3 = \sigma_z = \begin{pmatrix} 1 & 0 \\ 0 & -1 \end{pmatrix} \tag{B.9}$$

$$S = \begin{bmatrix} a_+ & 0 & 0 & a_- \\ 0 & a_+ & a_- & 0 \\ 0 & a_- & a_+ & 0 \\ a_- & 0 & 0 & a_+ \end{bmatrix} \tag{B.10}$$

where

$$a_\pm = \pm\sqrt{\frac{1}{2}(\gamma \pm 1)} \tag{B.11}$$

this $\gamma = 1/\sqrt{1 - v^2/c^2}$ where $\sigma^{\mu\nu} = \frac{i}{2}(\gamma^\mu\gamma^\nu - \gamma^\nu\gamma^\mu)$

B.2 Feynman Rules for QED

Similarly to the most basic of the scattering interactions, the process for calculating QED interactions involves the same sequence of steps.

1. Once again, label all incoming and outgoing momenta with p_i and all internal momenta with q_i

2. Now each vertex contributes a factor $ig_e\gamma^\mu$ where $g_e = e\sqrt{4\pi/\hbar c}$ and e is the charge of the electron. And again, each vertex is assigned a delta function, $(2\pi)^4\delta^4(k_1 + k_2 + k_3)$, to conserve energy and momentum

3. Unlike before, the propogators for mediator particles in QED are the following:

$$\frac{i(\gamma^\mu q_\mu + mc)}{q^2 - m^2c^2} \quad \text{for electrons and positrons}$$
$$\frac{-ig_{\mu\nu}}{q^2} \quad \text{for photons}$$

   And each internal momenta contributes a $d^4q/(2\pi)^4$

4. each incoming or outgoing particle contribute the following factors dependent on their identity:

$$\text{Electrons :} \quad \begin{cases} \text{Incoming: } u \\ \text{Outgoing: } \bar{u} \end{cases}$$

$$\text{Positrons :} \quad \begin{cases} \text{Incoming: } \bar{v} \\ \text{Outgoing: } v \end{cases}$$

$$\text{Photons :} \quad \begin{cases} \text{Incoming: } \epsilon_\mu \\ \text{Outgoing: } \epsilon^*_\mu \end{cases}$$

Note that the electrons and positrons are simply stand-ins for any lepton particle and anti-particle pair, excluding neutrinos.

5. The next sets are the same as before: integrate over the internal momenta and compute $\mathcal{M}$

6. The final new rule, is the rule of antisymmetrization. This rule means that a minus sign must be included between diagrams that differ only in the incoming or outgoing leptons

The final part of QED that will be useful in NC neutrino scattering is actually a mathematical trick that makes finding $\mathcal{M}$ much simpler: *Casimir's Trick*.

$$\sum_{all\ spins} [\bar{u}(a)\Gamma_1 u(b)][\bar{u}(a)\Gamma_2 u(b)]^* = Tr[\Gamma_1(\not{p}_b + m_b c)\bar{\Gamma}_2(\not{p}_a + m_a c)] \tag{B.12}$$

where "Tr" is simply the trace of the matrix.

Adding the electrodynamics formalism to the Feynman calculus helps to make the final cross-section expression more accurate, however it still will not be a complete picture of the event without taking into account the role chromodynamics plays in neutrino-nucleon interactions.

B.3 Quantum Chromodynamics

The structure of chromodynamics is similar to that of electrodynamics, but *color* takes the place of charge. Another important distinction between QED and QCD is that

charge only comes as a single number which is either positive or negative, whereas, there are three kinds of color: red, blue, and green, which adds greater complications.

Since quarks and, by extension, gluons can come in various colors and flavors, the coupling constant that is one value for QED varies in QCD. It is determined by the relative relationship between the number of flavors versus colors present:

$$a \equiv 2f - 11n \tag{B.13}$$

where f is the number of flavors and n is the number of colors. At short distances, this causes an increase in the coupling constant if there are more flavors and a decrease if there are more colors.

For the purposes of the later derivation of the cross-section, the values from the standard model are used where $f = 6$ and $n = 3$. This give a coupling value of a = -21, meaning the QCD coupling decreases at short distances.

B.4 Feynman Rules for QCD

In Feynman calculus, the full coupling constant is expressed as a function of a:

$$g_s = \sqrt{4\pi a_s} \tag{B.14}$$

Like in QED, the specification of the particle's state will be given with a Dirac spinor. However, now that color is involved, there needs to be an addition three-element column vector that tells whether the color is red, blue, or green:

$$c = \begin{pmatrix} 1 \\ 0 \\ 0 \end{pmatrix} \text{ for red,} \qquad \begin{pmatrix} 0 \\ 1 \\ 0 \end{pmatrix} \text{ for blue, and} \qquad \begin{pmatrix} 0 \\ 0 \\ 1 \end{pmatrix} \text{ for green} \tag{B.15}$$

1. For *external lines*, if it is a quark/antiquark:

$$\text{Quarks}: \begin{cases} \text{Incoming: } u^{(s)}(p)c \\ \text{Outgoing: } \bar{u}^{(s)}(p)c^{\dagger} \end{cases}$$

$$\text{Anti-quarks}: \begin{cases} \text{Incoming: } \bar{v}^{(s)}(p)c^{\dagger} \\ \text{Outgoing: } v^{(s)}(p)c \end{cases}$$

if it is a gluon:

$$\text{Gluon}: \begin{cases} \text{Incoming: } \epsilon_{\mu}(p)a^{\alpha} \\ \text{Outgoing: } \epsilon^{*}_{\mu}(p)a^{\alpha *} \end{cases}$$

2. Each *internal line*, gives a factor of:

$$\text{Quarks and Anti-quarks: } \frac{i(\not{q} + mc)}{q^2 - m^2c^2}$$

$$\text{Gluons: } \frac{-ig_{\mu\nu}\delta^{\alpha\beta}}{q^2}$$

3. Each *vertex* has a factor of:

$$\text{Quark-Gluon: } \frac{-ig_s}{2}\lambda^{\alpha}\gamma^{\mu}$$

In this case,om itting any all gluon only vertexes since they are not needed for this upcoming derivation.

It is also useful to define the Gell-Mann "λ-matrices", which are as follows:

$$\lambda^1 = \begin{pmatrix} 0 & 1 & 0 \\ 1 & 0 & 0 \\ 0 & 0 & 0 \end{pmatrix} \qquad \lambda^2 = \begin{pmatrix} 0 & -i & 0 \\ i & 0 & 0 \\ 0 & 0 & 0 \end{pmatrix} \qquad \lambda^3 = \begin{pmatrix} 1 & 0 & 0 \\ 0 & -1 & 0 \\ 0 & 0 & 0 \end{pmatrix}$$

$$\lambda^4 = \begin{pmatrix} 0 & 0 & 1 \\ 0 & 0 & 0 \\ 1 & 0 & 0 \end{pmatrix} \qquad \lambda^5 = \begin{pmatrix} 0 & 0 & -i \\ 0 & 0 & 0 \\ i & 0 & 0 \end{pmatrix} \qquad \lambda^6 = \begin{pmatrix} 0 & 0 & 0 \\ 0 & 0 & 1 \\ 0 & 1 & 0 \end{pmatrix}$$

$$\lambda^7 = \begin{pmatrix} 0 & 0 & 0 \\ 0 & 0 & -i \\ 0 & i & 0 \end{pmatrix} \qquad \lambda^8 = \frac{1}{\sqrt{3}} \begin{pmatrix} 1 & 0 & 0 \\ 0 & 1 & 0 \\ 0 & 0 & -2 \end{pmatrix}$$

B.5 Weak Interactions

The final step that needs to be explained before attempting to create a full expression for the neutrino-proton scattering cross-section is the effects of the weak interaction. In Chapter 2 , the theory of electroweak interaction is explored more in depth, however the mathematical breakdown of it's application in Feynman calculus will be outlined here.

Just like interactions in QED or QCD, weak interactions have mediator particles however the W and Z boson have mass, unlike the photon and gluon which are massless. This changes the propagator element to:

$$\frac{-ig_{\mu\nu} - q_\mu q_\nu / M^2c^2}{q^2 - M^2c^2} \tag{B.16}$$

For processes where the q^2 energies are much less that $(Mc)^2$ this can be simplified to:

$$\frac{-ig_{\mu\nu}}{M^2c^2} \tag{B.17}$$

Since, the work done in this thesis specifically focuses on neutral-current interactions, I have chosen to omit the formalism for charged-current theory.

Once again, interaction vertexes contribute a factor specific to weak processes:

$$\frac{-ig_z}{2}\gamma^\mu(c_V^f - c_A^f\gamma^5) \tag{B.18}$$

where $g_z = g_e/(\sin\theta_w\cos\theta_w)$, $g_e = e\sqrt{4\pi/\hbar c}$, and $\theta_w = 28.75°$.

f	c_V	c_A
ν_e, ν_μ, ν_τ	$\frac{1}{2}$	$\frac{1}{2}$
e^-, μ^-, τ^-	$-\frac{1}{2} + 2\sin^2\theta_w$	$-\frac{1}{2}$
u,c,t	$\frac{1}{2} - \frac{4}{3}\sin^2\theta_w$	$\frac{1}{2}$
d,s,b	$-\frac{1}{2} + \frac{2}{3}\sin^2\theta_w$	$-\frac{1}{2}$

Appendix C

Differential cross-section for elastic NC neutrino-proton scattering

Just like in Appendix A, the Feynman diagram structure is the same, however, calculating the cross-section is more complicated once incorporating the QED and QCD formalism.

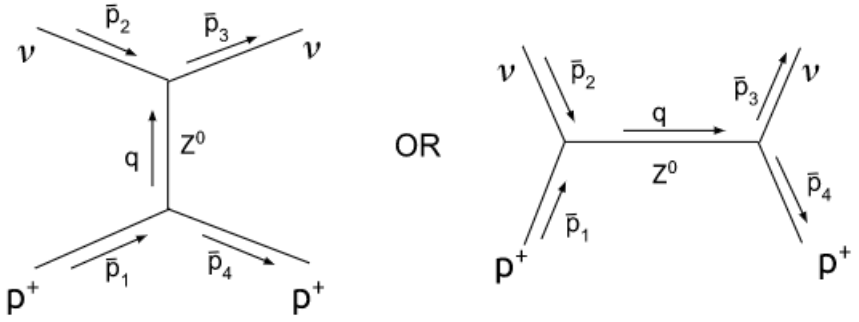

FIGURE C.1: Possible Feynman diagrams for ν-p^+ scattering

After establishing the possible diagrams for the interaction, the first step in the process is the same as before: labelling the incoming, outgoing, and internal momenta with their respective indices. For the second, step it is now necessary to classify the involved particles based on their SM class and force by which they interact.

For neutrino-proton elastic scattering, there is an electroweak interaction. This means that there will be components of both QED and QCD terms in the mixing matrix expression. And, since the interaction is mediated via the Z-boson it is imperative that

the correct propagator factor is used. Back in Appendix B.3, it was stated the the for q^2 energies much less that (Mc^2) the propagator can be greatly simplified; in this derivation, this initial assumption is made since the value $(M_Z c)^2$ is large. The factor we get is:

$$\frac{-ig_{\mu\nu}}{(M_Z c)^2} \tag{C.1}$$

Since there are two vertexes of interaction, there will be a factor of the QCD weak process vertex factors, assigned to the interaction vertex of the neutrino with the Z-boson:

$$\frac{-ig_Z}{2}\gamma^\mu(c_V^f - c_A^f\gamma^5) \tag{C.2}$$

values for g_z, f, c_V, and c_A can be found on page 54.

For the vertex where the proton and Z-boson interact, there is still QCD involved and so that vertex gets assigned the factor:

$$\frac{-ig_s}{2}\lambda^\alpha\gamma^\mu \tag{C.3}$$

The λ-matrices can be found on page 53.

Other factors that contribute to the mixing matrix include:

1. $u^{(s_1)}(p_1)c$ for the incoming proton, $\bar{u}^{(s_4)}(p_4)c^\dagger$ for the outgoing proton
2. $v^{(s_2)}(p_2)c$ for the incoming neutrino, $\bar{v}^{(s_3)}(p_3)c^\dagger$ for the outgoing neutrino
3. $(2\pi)^4\delta^4(p_1 - p_4 - q)$ and $(2\pi)^4\delta^4(p_2 - p_3 + q)$ where q$\equiv p_1 - p_4$ or $p_3 - p_2$ from conservation of momentum
4. the internal line gets $d^4q/(2\pi)^4$

Combining this will give the expression used to determine the mixing matrix, $\mathcal{M}$, via the same set of steps show in earlier appendices. Once $\mathcal{M}$ is found, Casimir's trick will be used to determine $\langle|\mathcal{M}|\rangle^2$, before creating the final expression for the cross-section.

Diagram A

$$-i(2\pi)^4\mathcal{M}_A = \int [\bar{u}^{(s_4)}(p_4)c^\dagger \left\{\frac{-ig_s}{2}\lambda^\alpha\gamma^\mu\right\} u^{(s_1)}(p_1)c][\bar{v}^{(s_3)}(p_3)c^\dagger \left\{ig_Z\gamma_\mu(c_V - c_A\gamma^5)\right\} v^{(s_2)}(p_2)c]$$
$$\times \left(\frac{ig_{\mu\nu}}{(M_Zc)^2}\right)(2\pi)^4\delta^4(p_2 - p_3 + q)(2\pi)^4\delta^4(p_1 - p_4 - q)\frac{d^4q}{(2\pi)^4}$$

Letting q=p_1-p_4, the R.H.S becomes:

$$(2\pi)^4\left\{\frac{(-ig_s)(ig_z)}{2(M_Zc)^2}\right\}\int [\bar{u}^{(s_4)}(p_4)c^\dagger \left\{\lambda^\alpha\gamma^\mu\right\} u^{(s_1)}(p_1)c]\,(ig_{\mu\nu})\,[\bar{v}^{(s_3)}(p_3)c^\dagger$$
$$\times \left\{\gamma_\mu(c_V - c_A\gamma^5)\right\} v^{(s_2)}(p_2)c]\delta^4(p_1 + p_2 - p_3 - p_4)d^4(p_1 - p_4)$$
$$= i(2\pi)^4\left\{\frac{g_sg_z}{2(M_Zc)^2}\right\}[\bar{u}^{(s_4)}(p_4)c^\dagger \left\{\lambda^\alpha\gamma^\mu\right\} u^{(s_1)}(p_1)c]$$
$$\times[\bar{v}^{(s_3)}(p_3)c^\dagger \left\{\gamma_\mu(c_V - c_A\gamma^5)\right\} v^{(s_2)}(p_2)c]$$

This gives:

$$\mathcal{M}_A = -\frac{g_sg_z}{2(M_Zc)^2}[\bar{u}^{(s_4)}(p_4)c^\dagger \left\{\lambda^\alpha\gamma^\mu\right\} u^{(s_1)}(p_1)c][\bar{v}^{(s_3)}(p_3)c^\dagger \left\{\gamma_\mu(c_V - c_A\gamma^5)\right\} v^{(s_2)}(p_2)c]$$

Finding $\langle|\mathcal{M}|\rangle^2$:

$$\langle|\mathcal{M}|\rangle^2 = \left(\frac{g_sg_z}{2(M_Zc)^2}\right)^2 [\bar{u}^{(s_4)}(p_4)c^\dagger \left\{\lambda^\alpha\gamma^\mu\right\} u^{(s_1)}(p_1)c][\bar{v}^{(s_3)}(p_3)c^\dagger \left\{\gamma_\mu(c_V - c_A\gamma^5)\right\} v^{(s_2)}(p_2)c]$$
$$\times[\bar{u}^{(s_4)}(p_4)c^\dagger \left\{\lambda^\alpha\gamma^\mu\right\} u^{(s_1)}(p_1)c]^*[\bar{v}^{(s_3)}(p_3)c^\dagger \left\{\gamma_\mu(c_V - c_A\gamma^5)\right\} v^{(s_2)}(p_2)c]^*$$

To use Casimir's trick define:

$$G_1 \equiv [\bar{u}^{(s_4)}(p_4)c^\dagger \left\{\lambda^\alpha\gamma^\mu\right\} u^{(s_1)}(p_1)c][\bar{u}^{(s_4)}(p_4)c^\dagger \left\{\lambda^\alpha\gamma^\mu\right\} u^{(s_1)}(p_1)c]^*$$

where

$$[\bar{u}^{(s_4)}(p_4)c^\dagger \left\{\lambda^\alpha\gamma^\mu\right\} u^{(s_1)}(p_1)c]^* = [(u^{(s_4)}(p_4)c^\dagger)^\dagger\gamma^0 \left\{\lambda^\alpha\gamma^\mu\right\} u^{(s_1)}(p_1)c]^\dagger$$
$$= \bar{u}^{(s_1)}(p_1)c\,\gamma^0 \left\{\lambda^\alpha\gamma^\mu\right\}^\dagger \gamma^0u^{(s_4)}(p_4)c^\dagger$$

The same can be done if G_2 is defined as the following:

$$G_2 \equiv [\bar{v}^{(s_3)}(p_3)c^\dagger \left\{\gamma_\mu(c_V - c_A\gamma^5)\right\} v^{(s_2)}(p_2)c][\bar{v}^{(s_3)}(p_3)c^\dagger \left\{\gamma_\mu(c_V - c_A\gamma^5)\right\} v^{(s_2)}(p_2)c]^*$$

where

$$[\bar{v}^{(s_3)}(p_3)c^\dagger \left\{\gamma_\mu(c_V - c_A\gamma^5)\right\} v^{(s_2)}(p_2)c]^* = \bar{v}^{(s_2)}(p_2)c\,\gamma^0 \left\{\gamma_\mu(c_V - c_A\gamma^5)\right\} \gamma^0 u^{(s_3)}(p_3)c^\dagger$$

Casimir's trick says that:

$$\sum_{all\ spins} G_1 = \mathrm{Tr}[\lambda^\alpha\gamma^\mu(\not{p_1} + m_1c)\gamma^0(\lambda^\alpha\gamma^\nu)^\dagger\gamma^0(\not{p_4} + m_4c)]$$

$$\sum_{all\ spins} G_2 = \mathrm{Tr}[\gamma_\mu(c_V - c_A\gamma^5)(\not{p_2} + m_2c)\gamma^0(\gamma_\nu(c_V - c_A\gamma^5))^\dagger\gamma^0(\not{p_3} + m_3c)]$$

Omitting the tedious algebra, these summations can be manipulated into the forms:

$$\sum_{all\ spins} G_1 = 4\lambda^\alpha\lambda^{\alpha\dagger}\left(p_1^\mu p_4^\nu + p_4^\mu p_1^\nu + g^{\mu\nu}[m_1m_4c^2 - (p_1 \cdot p_4)]\right)$$

$$\sum_{all\ spins} G_2 = 4(c_V^2 + c_A^2)\left(p_{2\mu}p_{3\nu} + p_{3\mu}p_{2\nu} - g_{\mu\nu}[m_2m_3c^2 - (p_2 \cdot p_3)]\right)$$

Substituting them into their respective parts of the mixing matrix, the following expression is obtained:

$$\langle|\mathcal{M}_A|\rangle^2 = 16\lambda^\alpha\lambda^{\alpha\dagger}(c_V^2 + c_A^2)\left(\frac{g_sg_z}{2(M_zc)^2}\right)^2 (p_1^\mu p_4^\nu + p_4^\mu p_1^\nu + g^{\mu\nu}[m_1m_4c^2 - (p_1 \cdot p_4)])$$
$$\times(p_{2\mu}p_{3\nu} + p_{3\mu}p_{2\nu} - g_{\mu\nu}[m_2m_3c^2 - (p_2 \cdot p_3)]) \tag{C.4}$$

The constant λ^α is a collection of matrices called Gall-Mann "A-matrices" and are the SU(3) analogous version of the Pauli spin matrices in SU(2).

Diagram B

One of the most important aspects of using Feynman calculus to derive the scattering cross-section is to consider all possible versions of the interaction. However, in this case, it is unnecessary to consider anything other that Diagram A because the type

of interaction doesn't allow for scattering in the way that Diagram B represents. Diagram B shows the decay of a proton and neutrino into a Z-boson, however this is not physically possible so it can be disregarded. Allowing the final mixing matrix to only have the contributions of Diagram A.

The mixing matrix is just one element of the full cross-section expression, but it is also the most tedious derive. Now that it has been found, it is relatively easy to piece everything together.

Appendix D

Python script for data filtering

After loading the file, some contained information about the run number and event number and this allowed us to examine multiple particles within a single event. However, it was soon discovered that during the MINERνA data collection process event number were often recycled, so hits were being grouped together by the python script that shouldn't have been. To alleviate this obstacle, a script was created to create unique event numbers using particle run and line numbers.

```
[ ]  #make event unique by adding run number to the beginning

     def add_runandevent(x, y):
       f = x + y * 10000000
       return f

     df["event"] = add_runandevent(df["event"], df["run #"])
```

```
[ ]  df.head()
```

	line #	run #	event	ipdg	px	py	pz	Energy	x	y	z	t
0	1	6192	6258886796679	13	-997.3590	-1282.2800	4333.1300	4628.840	384.44900	2.72221	-208.7670	-997.359
1	1	6192	6258886796679	2112	568.2910	357.7320	1192.6400	1660.160	-269.39400	-499.53100	43.0712	-1282.280
2	1	6192	6258886796679	211	11.3004	-15.7903	10.3325	141.293	8670.31000	8472.19000	-22.8988	4333.130
3	1	6192	6258886796679	2112	115.8380	-198.7250	15.2593	967.437	2586.45000	8486.90000	930.6650	4628.840
4	1	6192	6258886796679	211	253.1280	431.4970	2935.1200	2980.720	2.72221	-208.76700	-997.3590	0.000

```
[ ]  #assign the same line numbers to all the hits in the same event
     newarray=[]
     for index in df1.index:

       #this gets rid of the correction at the beginning of the list
       if index != ni:
         y = index - 1
       else:
         y = index


       if df1.loc[index, "event"] != df1.loc[y, "event"]: #if the new line index doesn't equal the on before it, append the number using the line number from before
         eventnumber = df1.loc[index, "event"]
         #print(eventnumber)
         help = np.where(df1["event"] == eventnumber) #this gives the index of all the lines with the eventnumber
         #print(help)
         help1 = pd.DataFrame.transpose(pd.DataFrame(help)) #compiles them into a dataframe
         #print(help1)
         for index in help1.index:
           i = help1[0].iloc[0] #first line index with that new event number
           linenumber = df1.loc[i, "line #"] #gives the line number(from the original dataframe) associated with that event number
           newarray.append(linenumber)
```

```
[ ]  #add the new line # to the end of the event number to make each one completely unique for each actual event
     df1["event"] = df1["event"] *100 + df1["new line"]
```

This part of the script only needs to be run for data files with non-unique event numbers. To determine if a file fits this criteria, simply model number of muons per event number; if it outputs counts greater than five mostly likely it is accounting for multiple files with the same event number. After creating unique event numbers we can group by them to look at individual events.

```
[ ]  #group all of the info by event into a new dataframe
     new_event_number_count =  df.groupby('event')
     df2= pd.DataFrame(new_event_number_count)
     df2.head()
```

```
     muoncount_array = []
     other_array = []
     neutroncount_array = []
     pioncount_array = []
     for i in range(len(df2)) :
       #print("Event Number: ", events.iloc[i,0])
       #print(events.iloc[i,1])

       #These next lines assign each column of the dataframe to their own array so they can be plotted later
       array_event = np.array(df2.iloc[i,0])
       array_info = np.array(df2.iloc[i,1]) # linenumber, indexnumber, runnumber, event, ipdg, px, py, pz, energy, x, y, z, t
       #print(array_info)
       count_electron = np.count_nonzero(array_info == 11)
       count_muon = np.count_nonzero(array_info == 13)
       count_antimuon = np.count_nonzero(array_info == -13)
       count_neutron = np.count_nonzero(array_info == 2112)
       count_proton = np.count_nonzero(array_info ==2212)
       count_pion = np.count_nonzero(array_info == 111)
```

```
       #These next lines append whatever arrays I'm currently interested in with the most current data
       muoncount_array.append(count_muon)
       neutroncount_array.append(count_neutron)
       pioncount_array.append(count_pion)
```

We wanted to look at the scattering angle distribution based on particle energy. To do that we first need to determine the particle's momentum in the beamline reference frame, where momentum in the files is w.r.t the detectors reference frame. This can be done using rotation matrices since we know that the angle between the two is 3.34°.

```
[ ] theta = 0.058 #radians
    rotation_matrix = np.array([[1, 0, 0], [0, np.cos(theta), -1*np.sin(theta)], [0, np.sin(theta), np.cos(theta)]])

    dfvertex.head()
    pxf = 1 * dfvertex["px"]
    pyf = dfvertex["py"]* np.cos(theta)+ np.sin(theta) * dfvertex["pz"]
    pzf = -1 * dfvertex["py"]* np.sin(theta)+ np.cos(theta) * dfvertex["pz"]
```

```
[ ] dfvertex["pxf"] = pxf
    dfvertex["pyf"] = pyf
    dfvertex["pzf"] = pzf
```

```
[ ] momentum = pd.DataFrame(dfvertex["pxf"])
    momentum["pyf"] = dfvertex["pyf"]
    momentum["pzf"] = dfvertex["pzf"]
    momentum["part"] = dfvertex["ipdg"]
    momentum["energy"] = dfvertex["E"]
```

```
[ ] #need to do coordinate transforms
    #in this case we're rotating about the x-axis where +x is coming out of the page

    theta = 0.058 #radians
    rotation_matrix = np.array([[1, 0, 0], [0, np.cos(theta), -1*np.sin(theta)], [0, np.sin(theta), np.cos(theta)]])
    #print(rotation_matrix)

    event_array = []
    part_array = []

    px_array = []
    py_array = []
    pz_array = []

    E_array = []

    other1_array = []

    for i in range(len(df2)) :

      #this starts by grabbing the data for each event, line by line
      grab = df2[1].iloc[i]

      for i in range(len(grab)):

        event = grab.iloc[i, 2]
        part = grab.iloc[i, 3]
        pxi = grab.iloc[i, 4]
        pyi = grab.iloc[i, 5]
        pzi = grab.iloc[i, 6]
        Ei = grab.iloc[i, 7] #this energy is in GeV and includes the rest mass energy of the particle
```

```
[ ]       initial_mom_array = np.array([pxi, pyi, pzi])
          final_mom_array = np.dot(rotation_matrix, initial_mom_array)



          pxf = final_mom_array[0]
          pyf = final_mom_array[1]
          pzf = final_mom_array[2]

          part_array.append(part)
          px_array.append(pxf)
          py_array.append(pyf)
          pz_array.append(pzf)
          E_array.append(Ei)
          event_array.append(event)
```

```
momentum = pd.DataFrame(px_array, columns = ["px"])
momentum["py"] = py_array
momentum["pz"] = pz_array
momentum["Total E"] = E_array
momentum["event"] = event_array
momentum["particle"] = part_array
```

Next, we apply this to all hits as well as finding the kinetic energy for each particle. The energy in the files is made up of both rest mass energy and kinetic.

```
[ ]  trial = []
     mag = []
     theta_beam = []

     for i in range(len(momentum)):
       trial1 = momentum.iloc[i]
       mag1 = (trial1[0]**2 + trial1[1]**2 + trial1[2]**2) ** (1/2)

       #calculating theta, wrt the beam axis
       theta_beam1 = 180/np.pi *np.arccos(trial1[2]/mag1) #this is in degrees

       trial.append(trial1)
       mag.append(mag1)
       theta_beam.append(theta_beam1)
```

```
[ ]  #trial run
     x = momentum

     rme_neutron = 0.9396 #gev
     rme_proton = 0.938 #gev
     rme_electron = 0.000511 #gev
     rme_muon = 0.1057 #gev
     rme_pion = 0.14 #gev
     rme_kaon = 0.493677 #gev

     ef_array = []

     for i in range(len(x)):
       x1 = x["Total E"].iloc[i] #grabs the energy column
       x2 = x["particle"].iloc[i] #grabs the particle column
       #print(i, x1, x2)

       if np.absolute(x2) == 2212:
         ef = x1 - rme_proton
         #print(i, "this is a proton", ef)

       if np.absolute(x2) == 11:
         ef = x1 - rme_electron
         #print(i, "this is an electron", ef)

       if np.absolute(x2) == 2112:
         ef = x1 - rme_neutron
         #print(i, "this is a neutron", ef)

       if np.absolute(x2) == 13:
         ef = x1 - rme_muon
         #print(i, "this is a muon", ef)
```

```
[ ]    if np.absolute(x2) == 130:
         ef = x1 - rme_kaon

       if np.absolute(x2) == 211:
         ef = x1 - rme_pion

       else:
         ef = x1

       ef_array.append(ef)
```

```
[ ]  momentum["theta"] = theta_beam
     momentum["Kinetic Energy"] = ef_array
     #2212 are protons
```

```
[ ]  newarray3 = []

     for i in range(len(momentum)):
       if momentum["Kinetic Energy"].iloc[i] >= 99.999:
         newarray3.append(momentum.iloc[i])

     newarray4 = np.array(newarray3)
     newarray5 = []
     for i in range(len(newarray4)):
       if newarray4[i,7] <= 10000:
         newarray5.append(newarray4[i])
```

```
[ ]  df4 = pd.DataFrame(newarray5, columns = ["px", "py", "pz", "E", "event", "particle", "theta", "Kinetic Energy"])
```

```
[ ]  #this takes the hits and grads only the muons, and their angle and kinetic energy
     newarray6 = np.array(df4)
     energy1 = []
     theta1 = []
     ipdg1 = []

     for i in range(len(df4)):
       if np.absolute(df4.iloc[i,5]) == 13:
         energy1.append(df4.iloc[i,7])
         theta1.append(df4.iloc[i,6])
         ipdg1.append(df4.iloc[i,5])

     plot2 = np.array(list(zip(energy1, theta1, ipdg1)))
     df5_1 = pd.DataFrame(plot2)
```

```
[ ]  #plotting scattering angle as a function of incident energy

     import matplotlib as mpl
     from matplotlib import pyplot as plt, colors
     fig, ax = plt.subplots()
     hh = ax.hist2d(df5_1[0],df5_1[1], bins=25, norm=colors.LogNorm())
     fig.colorbar(hh[3], ax=ax)
     plt.xlabel("Energy (GeV)" )
     plt.ylabel("${\Theta}_{wrt\,beam\,axis}$ (degrees)")
     plt.title("Scattering Angle Distribution for Downstream ECAL (FHC)")
     plt.show()

     print("this plot only includes energy levels from 100MeV to 10 GeV")
```

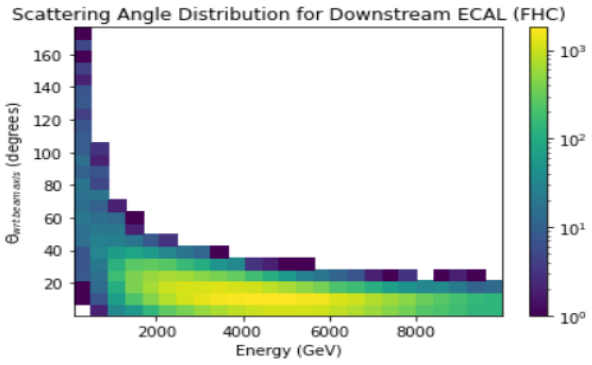

Bibliography

[1] Standard model. https://en.wikipedia.org/wiki/Standard_Model, . Accessed: 2022-06-11.

[2] J. Formaggio and G. Zeller. From ev to eev: Neutrino cross sections across energy scales. *Reviews of Modern Physics*, 84, 05 2013. doi: 10.1103/RevModPhys.84.1307. URL https://www.researchgate.net/publication/236985384_From_eV_to_EeV_Neutrino_Cross_Sections_Across_Energy_Scales.

[3] Minerνa: How it works. https://minerva.fnal.gov/how-it-works/, .

[4] Laurie M. Brown. The idea of the neutrino. *Physics Today*, 31(9):23–28, September 1978. doi: 10.1063/1.2995181.

[5] The T2K Collaboration. A brief history of neutrinos. https://t2k-experiment.org/neutrinos/a-brief-history/.

[6] Prehistory and birth of the neutrino. https://neutrino-history.in2p3.fr/prehistory-and-birth-of-the-neutrino/, . Accessed: 2022-06-11.

[7] David Griffiths. *Introduction to Elementary Particles*. Wiley-VCH, 2008. URL https://mikefragugliacom.files.wordpress.com/2016/12/introduction-to-elementary-particles-gnv64.pdf.

[8] F. Reines and C. Cowan. The Reines-Cowan experiments: Detecting the Poltergeist. *Los Alamos Sci.*, 25:4–27, 1997.

[9] D. Perevalov, R. Tayloe, and et al. Measurement of neutrino-nucleon neutral current elastic scattering in MiniBooNE. In *AIP Conference Proceedings*. AIP, 2009. doi: 10.1063/1.3274151. URL https://doi.org/10.1063%2F1.3274151.

[10] V. Barger, D. Marfatia, and K. Whisnant. *The Physics of Neutrinos*. Princeton University Press, 2012.

[11] Carlotta Giusti and Martin V Ivanov. Neutral current neutrino-nucleus scattering: theory. *Journal of Physics G: Nuclear and Particle Physics*, 47(2):024001, jan 2020. doi: 10.1088/1361-6471/ab5251. URL https://doi.org/10.1088/1361-6471/ab5251.

[12] L. P. Pitaevskii V. B. Berestetskii, E.M. Lifshits. *Relativistic Quantum Theory*. Pergamon Press, 1971.

[13] Xianhao Xin. Glashow-weinberg-salam model: An example of electroweak symmetry breaking. 2007.

[14] L. Aliaga, L. Bagby, and et al. Design, calibration, and performance of the minerva detector. *Nuclear Instruments and Methods in Physics Research Section A: Accelerators, Spectrometers, Detectors and Associated Equipment*, 743:130–159, 2014. ISSN 0168-9002. doi: https://doi.org/10.1016/j.nima.2013.12.053. URL https://www.sciencedirect.com/science/article/pii/S0168900214000035.

[15] K.S. McFarland. Minerνa: a dedicated neutrino scattering experiment at numi. *Nuclear Physics B - Proceedings Supplements*, 159:107–112, 2006. ISSN 0920-5632. doi: https://doi.org/10.1016/j.nuclphysbps.2006.08.073. URL https://www.sciencedirect.com/science/article/pii/S0920563206005159. Proceedings of the 4th International Workshop on Neutrino-Nucleus Interactions in the Few-GeV Region.

[16] How to make a neutrino beam. https://www.symmetrymagazine.org/article/november-2012/how-to-make-a-neutrino-beam, .

[17] C. Andreopoulos, A. Bell, and et al. The GENIE neutrino monte carlo generator. *Nuclear Instruments and Methods in Physics Research Section A: Accelerators, Spectrometers, Detectors and Associated Equipment*, 614(1):87–104, 2010. ISSN 0168-9002. doi: https://doi.org/10.1016/j.nima.2009.12.009. URL https://www.sciencedirect.com/science/article/pii/S0168900209023043.

[18] Makoto Asai. Introduction to GEANT4. https://geant4.web.cern.ch/sites/default/files/geant4/support/training/CSC2000/CSCG4.pdf.

[19] G. Barrand, I. Belyaev, and et al. GAUDI — a software architecture and framework for building hep data processing applications. *Computer Physics Communications*, 140(1):45–55, 2001. ISSN 0010-4655. doi: https://doi.org/10.1016/S0010-4655(01)00254-5. URL https://www.sciencedirect.com/science/article/pii/S0010465501002545.

[20] M. Clemencic, H. Degaudenzi, and et al. Recent developments in the lhcb software framework gaudi. *Journal of Physics: Conference Series*, 219:042006, 05 2010. doi: 10.1088/1742-6596/219/4/042006. URL https://iopscience.iop.org/article/10.1088/1742-6596/219/4/042006.

[21] N. Tagg, J. Brangham, J. Chvojka, and et al. Arachne—a web-based event viewer for minera. *Nuclear Instruments and Methods in Physics Research Section A: Accelerators, Spectrometers, Detectors and Associated Equipment*, 676:44–49, June 2012. ISSN 0168-9002. doi: https://doi.org/10.1016/j.nima.2012.01.059. URL https://www.sciencedirect.com/science/article/pii/S0168900212001167.

[22] P. Hernandez. Neutrino physics. In *5th CERN - Latin American School of High-Energy Physics*, 10 2010. URL https://arxiv.org/pdf/1010.4131.pdf.